

Sediment Study in Storm Sewer Catchbasins and Submerged Pipes

by

Yangbo Tang

A thesis submitted in partial fulfillment of the requirements for the degree of

Master of Science

in

Water Resources Engineering

Civil and Environmental Engineering

University of Alberta

© Yangbo Tang, 2016

Abstract

Studying sediment in storm sewer systems is important for the operation and design of storm sewer systems. This thesis presents a literature review on the existing work on sediment in storm sewer, and conducts the experimental studies on sediment motion and settlement in storm sewer catchbasins and submerged pipes.

Sediment may pollute downstream water, adversely impacting aquatic life, source waters for drinking water supplies, and recreational uses. Sedimentation in sewer pipes may cause sewer blockage problems, reduce the flow area and cause surcharged flows and urban flooding. Storm sewer sediment characteristics reported in the literature include storm sewer sediment sources, classification based on sediment sizes, particle median size surveys, particle size distribution investigations, particle settling velocity calculations, and the particle pollution potentials.

During the rainfall, the sediment moves from catchment surface into storm sewer catchbasins, and then enters storm sewer pipes. Thus, related literature on sediment loading estimation and sediment movement in sewer pipes is included. A number of factors need to be considered in estimating sediment loading: sediment buildup, rainfall intensity, rainfall energy, runoff rate, sediment sizes, and land surface characteristics. Sediment movement includes three parts: erosion, transport and deposition. In terms of sediment blockage problems, sediment critical erosion velocity and sediment self-cleansing velocity are discussed in detail. Also, a collection of different experiments about sediment movement in storm sewers is presented.

A laboratory experiment was conducted to predict sediment removal efficiency in catchbasins under different conditions (including flow rate, particle size, and inlet control device). For Calgary's catchbasins, particles with d_{50} of 1800 μm can be easily captured, while smaller particles of 62 μm d_{50} can be easily flushed out of catchbasins, even at low flow discharge. An equation is developed for predicting sediment capture efficiency in a catchbasin for different particle sizes and flow rates. The proposed equation can be used for catchbasin design.

Consequently, a laboratory experiment on sediment movement in submerged pipes was completed. According to the experimental observations, the development of deposition appears to occur over two distinct stages: the rapid developing stage (sand deposit grows both in height and in length directions), and the equilibrium developing stage (sand deposit only grows in the length direction). With respect to sediment transport capacity, it can be described by an equation consisting of a sediment transport parameter, bed shear intensity, and relative bed thickness.

Preface

Chapter 3 of this thesis has been submitted to the journal Water Science and Technology as “Experimental Study of Hydraulics and Sediment Capture Efficiency in Catchbasins” with the following authors: Yangbo Tang, David Z. Zhu, N. Rajaratnam, and Bert van Duin. I was responsible for the experimental design, data collection and analysis as well as the manuscript composition. David Z. Zhu was the supervisory author and was involved with concept formation and manuscript composition. N. Rajaratnam and Bert van Duin contributed to manuscript edits.

Acknowledgements

To begin I would like to express my deep gratitude to my supervisor Dr. David Z. Zhu. His thoughtful insight and scientific enthusiasm, support and guidance throughout my research study helped me during this incredible period of intellectual growth.

Secondly, I would like to thank Dr. Nallamuthu Rajaratnam for introducing me to sediment transport and for providing hydraulic modeling design guidance. Besides, he has inspired me to continuously improve my English writing skills. Also, I would also like to sincerely thank Bert Van Duin from City of Calgary for his collaborative contributions in the experiment design. A special thank you goes to Perry Fedun who helped to build all experimental arrangements in the hydraulic lab.

Finally, I would like to express my gratitude to my family and close friends for their support and encouragement during the period of my graduate studies.

Table of Contents

Abstract.....	ii
Preface.....	iv
Acknowledgements.....	v
List of Tables	ix
List of Figures	x
List of Symbols	xiii
Chapter 1: Introduction	1
1.1 Background.....	1
1.2 Objectives of the study.....	2
1.3 Scope of the study and structures of the thesis	3
Chapter 2: Literature Review.....	5
2.1 Storm sewer sediment characteristics	5
2.2 Storm sewer sediment wash-off load.....	11
2.3 Erosion	12
2.4 Transport.....	14
2.5 Deposition.....	19
2.6 A collection of experiments on sediment movement in storm sewers.....	23

2.7 Pollution potential.....	25
2.8 Summary.....	25
Chapter 3: Experimental Study of Hydraulics and Sediment Capture Efficiency in	
Catchbasins	27
3.1 Introduction.....	27
3.2 Methods.....	30
3.3 Hydraulics of the flow in the catchbasin.....	35
3.4 Sediment capture efficiency.....	37
3.5 Model for predicting sediment capture efficiency	40
3.6 Summary.....	45
Chapter 4: Experimental Study of Sediment Movement in a Submerged Pipe on Steep Slopes	
.....	48
4.1 Introduction.....	48
4.2 Experimental procedure	50
4.3 Single particle traveling velocity	53
4.4 Sediment deposition development	56
4.5 Sediment transport capacity	79
4.6 Summary.....	82

Chapter 5: Conclusions and Recommendations	84
5.1 Conclusions.....	84
5.2 Recommendations.....	86
References.....	89

List of Tables

Table 1. Sources of storm sewer sediment.....	5
Table 2. The median size, d_{50} , of deposit sediment found in storm sewer systems.....	10
Table 3. Various models in the literature for sewer sediment erosion motion	14
Table 4. Equations for sediment transport over rigid boundary	16
Table 5. Equations for sediment transport over loose boundary	17
Table 6. Sediment transport models developed in the literature based on ϕ and ψ	19
Table 7. Summary of experiments about sediment movement in storm sewers.....	24
Table 8. Metal distribution in different sizes of particles	25
Table 9. Sand information.....	33
Table 10. Experiment parameters for sediment removal efficiency in catchbasin	34
Table 11. A summary of sediment capture efficiency curves.....	45
Table 12. Particle information	51
Table 13. Experiment groups and tests	53
Table 14. Single particle relative traveling velocity equations.....	56
Table 15. Sediment bulk densities for 6.5 L/s flow rate scenario	58

List of Figures

Figure 1. Solids size classification diagram.....	7
Figure 2. Particle size distributions of sediment in stormwater runoff in different studies.....	8
Figure 3. Experimental setup and flow observations.....	31
Figure 4. An ICD installed in the outlet pipe, and ICD dimensions.....	32
Figure 5. Measured water depth and discharge relation in catchbasins.....	36
Figure 6. Energy dissipation rate in catchbasins.....	37
Figure 7. Sediment capture efficiency for different types of sand.....	41
Figure 8. Measured and simulated sediment capture efficiency in catchbasins	43
Figure 9. Experimental set up (unit: mm).....	51
Figure 10. Particle velocity measurements	54
Figure 11. Single particle relative traveling velocity.....	55
Figure 12. Sediment deposition volume plotted by AutoCAD.....	57
Figure 13. Sediment deposition development in height.....	60
Figure 14. Sediment deposition rapid develop stage (flow velocity 0.25 m/s and feeding rate 2.5 g/s).....	61
Figure 15. Sediment deposition development (including both rapid and equilibrium develop stages)	62
Figure 16. Sediment deposition in 0.5% pipe with 0.5 m/s flow velocity and 5 g/s sand feeding rate.....	63

Figure 17. Sediment deposition in 0.5% pipe with 0.5 m/s flow velocity and 15 g/s sand feeding rate.....	64
Figure 18. Sediment deposition in 0.5% pipe with 0.75 m/s flow velocity and 22 g/s sand feeding rate.....	65
Figure 19. Sediment deposition in 0.5% pipe with 0.75 m/s flow velocity and 45 g/s sand feeding rate.....	66
Figure 20. Sediment deposition in 1.0% pipe with 0.5 m/s flow velocity and 5 g/s sand feeding rate.....	67
Figure 21. Sediment deposition in 1.0% pipe with 0.5 m/s flow velocity and 15 g/s sand feeding rate.....	68
Figure 22. Sediment deposition in 1.0% pipe with 0.75 m/s flow velocity and 22 g/s sand feeding rate.....	69
Figure 23. Sediment deposition in 1.0% pipe with 0.75 m/s flow velocity and 45 g/s sand feeding rate.....	70
Figure 24. Sediment deposition in 2.0% pipe with 0.5 m/s flow velocity and 5 g/s sand feeding rate.....	71
Figure 25. Sediment deposition in 2.0% pipe with 0.5 m/s flow velocity and 15 g/s sand feeding rate.....	72
Figure 26. Sediment deposition in 2.0% pipe with 0.75 m/s flow velocity and 22 g/s sand feeding rate.....	73

Figure 27. Sediment deposition in 2.0% pipe with 0.75 m/s flow velocity and 45 g/s sand feeding rate.....74

Figure 28. Sediment deposition development in measured volume76

Figure 29. Sediment development rate changes with time78

Figure 30. Sediment transport parameter changes with dimensionless bed shear stress81

Figure 31. Sediment transport parameter changes with dimensionless bed thickness81

List of Symbols

Symbol	Definition
A'	Orifice area
A	Cross-section flow area
a	Rectangular orifice width
a_i & b_i	$i=1, 2, 3, \dots$ coefficient
b	Rectangular orifice height
$c, d, \text{ and } e$	Coefficient
C_1 C_2	Coefficient
C_d	Discharge coefficient
C_s	Ratio of sediment transport volume and flow rate
D	Pipe diameter
d_p	Particle size
d_{50}	Sediment median diameter
d^*	Dimensionless particle number
D_{in}	Inlet pipe diameter
D_{out}	Outlet pipe diameter
D_{gr}	Grain diameter in dimensionless term
F_j	Inflow jet Froude number
g	Acceleration due to gravity
h	Depth of water in the catchbasin above in the invert of the outlet pipe
H	Height of the inlet from the datum at the invert of the outlet pipe
ΔH	Head loss
h'	Water depth in the outlet pipe

i	$i = 1, 2, 3, \dots$
k	Particle absolute roughness
k_r	Relative pipe roughness
l	Water depth from water surface to structure bottom in the sump
P	Péclet number
q_b	Sediment transport rate per unit width
Q	Flow rate
R	Hydraulic radius
R_b	Hydraulic radius of the bed
s	Sediment specific gravity
S	Pipe slope
t	Time
T	Sediment thickness
T_r	Relative bed thickness
U^*	Bed shear velocity
V_m	Flow mean velocity
V_d	Deposition volume
V_c	Critical mean velocity
V_s	Self-cleansing velocity
V_p	Particle traveling mean velocity
V_{in}	Flow mean velocity in inlet pipe
V_{out}	Flow mean velocity in outlet pipe
V_v	Vertical mean velocity in the catchbasin
W	Sump width

W_b	Width of sediment bed
W_i	# i minute deposition development rate
w_s	Particle settling velocity
W_s	Sand addition rate
y	Water depth above the center of the orifice
y_0	Water depth in pipe
y_s	Deposit depth
Y	Flow depth in pipe
Y_r	Relative flow depth
Z	Relative grain size
λ_s	Overall friction factor
λ_{sb}	Deposit friction factor
λ_0	Pipe friction factor
ψ_b	Dimensionless bed shear stress
ϕ_b	Transport parameter
θ	Pipe tilting angle
η_E	Relative energy loss
η_S	Sediment capture efficiency
η_1	Transport coefficient
η^*	Rouse number
ρ_P	Particle density
ρ_b	Bulk density
ρ_w	Water density

Chapter 1: Introduction

1.1 Background

Stormwater sediments can cause many negative impacts on stormwater system receiving water bodies, and aquatic life. For stormwater systems, sediment deposition in sewers reduces flow area and can cause pipe blockage, consequently leading to surcharged flows and urban floods (Butler & Davies, 2011). As for the receiving water bodies, pollutants adhering to the sediment, including heavy metals, salt, hydrocarbons and high concentration of nutrients (e.g., Total Nitrogen and Total Phosphorus), pose direct threat to water quality (City of Calgary, 2011; USEPA, 1993). For aquatic lives, high level of sediment concentration contributes to high turbidity which limits sunlight penetration thereby prohibiting the growth of aquatic plants (Aryal and Lee, 2009). Also, sedimentation can clog fish spawning grounds.

The province of Alberta (Alberta Environment, 1999) stipulated that 85% of Total Suspended Solids (TSS) in stormwater should be removed before discharging into a receiving stream or river, through various stormwater management systems. City of Calgary developed a Stormwater Management Strategy in 2005 with the specific goal of reducing sediment loading to the Bow and Elbow Rivers from stormwater systems to 2005 levels by 2015 (Letourneau et al., 2008). Stormwater BMPs can help to realize the former targets, since stormwater BMPs are described as both structural or engineered control devices and systems to treat polluted stormwater. Thus, system inlets (catchbasins) are treated as objective stormwater BMPs to reduce sediment amounts entering storm sewer systems.

Storm sewer systems in Calgary include inlets (catchbasins), overland conveyance systems, underground pipe systems, ponds, outlets and Low Impact Development (City of Calgary, 2013). It should be mentioned that inlets (catchbasins) in Calgary are without sumps which leads to the addition of more sediment into storm sewer system instead of being captured in the sumps. Understanding the sediment removal efficiency in catchbasins can help to solve sedimentation problems in system outlets. According to historical records, many urban floods have occurred near storm sewer system outlets. Outlets to stormwater ponds are designed to be submerged in Calgary in order to avoid winter icing and odor problems. The higher water level in submerged pipes can reduce turbulence level and flow velocity, which contributes to serious sedimentation.

1.2 Objectives of the study

The without sump catchbasin design gives rise to questions as to that whether these storm sewer systems will suffer due to sedimentation. Thus, determining the sediment removal efficiency in different catchbasins is of great importance. After sediment entering the storm sewer system, most of it will be deposited near system outlets. Therefore, the sediment travelling velocity, sediment deposition development, and sediment transport capacity might be affected.

The objectivities of this study are as follows:

- a) To understand the sediment removal efficiency in catchbasins by testing the effect of flow rate, particle sizes, with and without sump, and inlet control device (ICD) with different openings.

- b) To understanding the sediment movement/deposition in submerged pipe by testing the effect of pipe slope and particle sizes.
- c) To recommend further research in this area.

1.3 Scope of the study and structures of the thesis

For the sediment removal efficiency study in catchbasins, the measurements are conducted in a system, from upstream to downstream, consisting of a sand & water feeding system, catchbasin and outlet pipe. In these experiments, water flow rate range is from 5 to 28 L/s, accordingly the sediment flux range is from 7.5 to 42 g/s. The D_{50} values of sediment particle sizes are 62, 100, 200, 250, 400 and 1800 μ . The ICD sizes are 50, 70, and 100 mm in diameter.

As for the sediment development study in submerged pipes, the experiment set-up is modified based on the former set-up. The modified system can be divided into three parts: a sand/water feeding system, a 6-m long 150 mm Plexiglas pipe and a downstream pond. In these sets of measurements, for single particle (0.5, 1, 2, and 4 mm) travelling velocity, different flow rates (6.5, 10.5, 13, 17, and 19.5 L/s) and pipe slopes (0.5, 1, and 2%) were tested. For the sediment deposition development and sediment transport experiments, (6.5 L/s in a 0.5% slope pipe), sand was added at a constant rate and the video started to record the deposition development. The test duration was 5 minutes. Different flow rates (6.5, 13 and 19.5 L/s), pipe slope (0.5%, 1% and 2%) and sand adding rates (2.5, 5, 15, 22, and 45 g/s) were tested.

This thesis is divided into five chapters. Chapter 2 reviews the literature on storm sewer sediment characteristics reported in the literature. Chapter 3 includes the study on sediment

capture efficiency in catchbasins. Chapter 4 presents the study on sediment deposition in a submerged pipe. Chapter 5 presents the important findings from the current study and also research outlook for the future.

Chapter 2: Literature Review

2.1 Storm sewer sediment characteristics

It is important to understand the origin and natural characteristics of in-sewer sediment. The nature of sediment solids (including origin, sizes and pollutant loads) has been researched extensively in the last couple of decades (Ashley *et al.*, 2005). In storm sewers, sediment mostly comes from a number of possible sources: atmospheric deposition, wash-off from the surfaces within the catchment, sewer pipes themselves and construction sites (Ashley & Hvitved-Jacobsen, 2002; Fan, 2004; Butler & Davies, 2011). Table 1 shows a summary of the sources of storm sewer sediment.

Table 1. Sources of storm sewer sediment (Ashley & Hvitved-Jacobsen, 2002; Fan, 2004; Butler & Davies, 2011)

Source	Particle characteristics	Description
Winter de-icing	Particle size range approximately from 0.05 to 20 mm	Sand or grit used for winter de-icing might be flushed into storm sewers.
Catchment surface	Wide size range, primary inorganic	Include grit from road abrasion, particulates from vehicles, construction materials, particles from erosion of roofing material, etc.)
Runoff from impervious areas	Typical solids <250 μm entering sewer carried by runoff	These solids may be up to 40% by mass of total storm sewer sediment load.
Soil erosion	Typical solids <1 mm	Due to leaks or pipe/manhole/gully failures
Wind-blown from sand/soil/litter	Large organics possible, inorganics <5 mm	Entry via catchbasins/inlets, size reduced when discharged into storm sewer due to the sediment capture ability in catchbasins/inlets

Due to the different sources of storm sewer sediments, these solids cover a size range from nanometer-sized colloidal organic material to millimeter-sized gravels. There are three classical grain size classifications for soils and sediments including the American Society for

Testing and Materials (ASTM D 2487, 1992), International Organization for Standardization (ISO 14688-1, 2002) and Wentworth (1922) grade scales. For ASTM D 2487:

- Coarse gravel: 19 mm – 75 mm;
- Fine gravel: 4.75 mm – 19 mm;
- Coarse sand: 2 mm – 4.75 mm;
- Medium sand: 0.475 mm – 2 mm;
- Fine sand: 0.075 mm- 0.475 mm;
- Clay or silt: < 0.475 mm.

The ISO 14688-1 (2002) and Wentworth (1922) scales are similar with the only difference being that Wentworth scale separates muds and fine sands at 62.5 μm . This classification is shown below:

- Gravel: > 2 mm;
- Coarse sand: 0.5 mm – 2 mm;
- Medium sand: 0.25 mm – 0.5 mm;
- Fine sand: 0.063 mm (or 0.0625 mm) – 0.25 mm;
- Mud: < 0.063 mm (or 0.0625 mm).

As for a more specific storm sewer sediment classification, Roesner and Kidner (2007) suggested a method for sediment classification in stormwater runoff based on particle size differences (Figure 1):

- Gross solids: > 5 mm (including coarse sand, gravel, and large debris);

- Coarse solids: defined as the solid material greater than 75 μm and less than 5 mm;
- Fine solids: defined as material that between 2 and 75 μm (including organic fine solids, silt, coarse clay, and phytoplankton);
- Dissolved solids: defined as the particles that smaller than 2 μm .

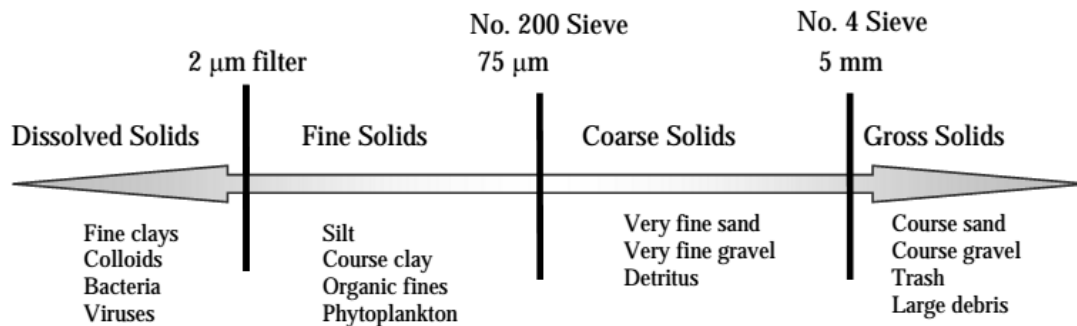


Figure 1. Solids size classification diagram (Roesner and Kidner, 2007)

However, this classification method is relatively new and no consistent classification for sediments in storm sewers has been reported in the literature. More studies are needed before its application.

Sediment size is an important part of sediment characteristics. The following section presents the sediment sizes in stormwater runoff and in the bottom deposit (in storm sewer inlets and sewers). Most studies have focused on the sediment size distribution in storm event water samples (stormwater runoff), that is, they used grab sampler or fixed point sampler to collect water samples. Figure 2 shows sediment size distributions collected from stormwater runoff in different areas.

Boogaard et al. (2014) measured particle size distribution in stormwater runoff in twenty-five locations in Netherland’s storm sewer system. Their results are plotted in Figure 2. As can be seen, half of the mass consists of particles smaller than 70 μm , which also means that particles are predominantly fine (60% of the particles are finer than 100 μm).

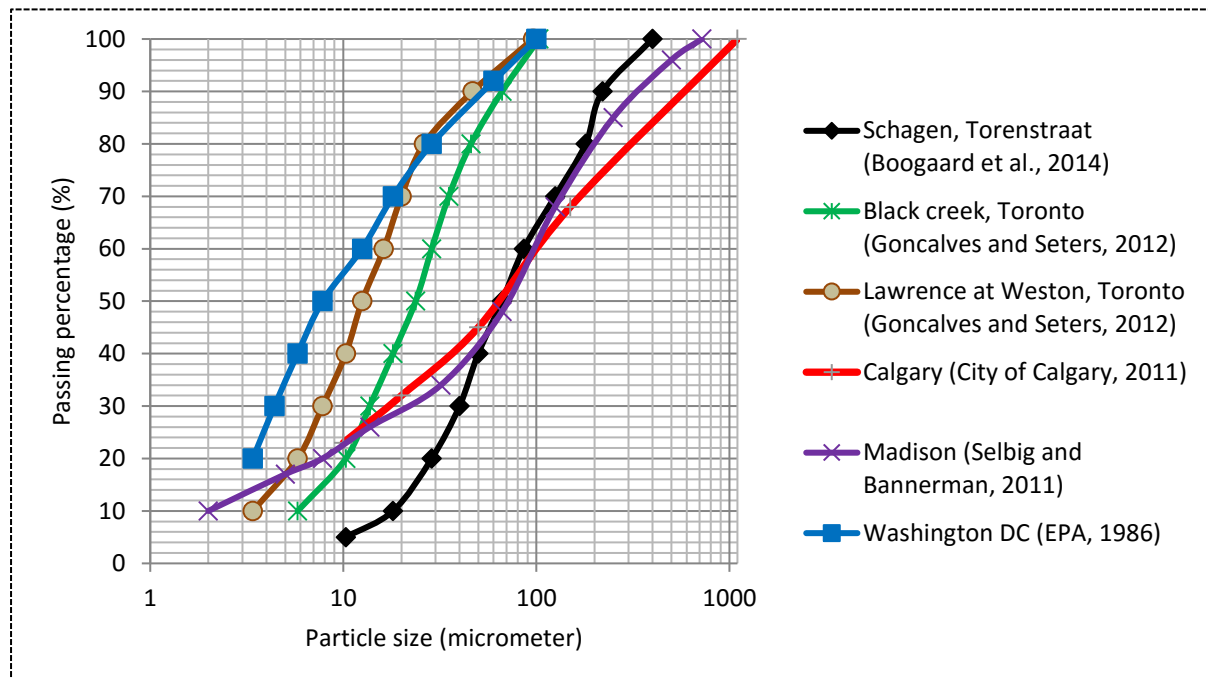


Figure 2. Particle size distributions of sediment in stormwater runoff in different studies.

Particle size distributions in two areas in Toronto were analyzed by Goncalves and Seters (2012). Though two sets of data were obtained in the same city, particle size distributions were different due to site specific features. Both sets were fine materials (50% of particles are finer than 13.7 μm in Lawrence at Weston and 90% of particles are finer than 55 μm in Black creek). A tendency similar to that in Toronto in particle size distribution was also reported in Washington DC (USEPA, 1986).

In Madison, Wisconsin, sediment from the mixed-use and parking-lot study areas had the lowest d_{50} of 42 and 54 μm , respectively, followed by the collector street study area with $d_{50}=70$ μm . Both arterial street and institutional roof study areas had similar d_{50} of 95 μm (Selbig and Bannerman, 2011). The particle size distribution in Calgary (City of Calgary, 2011) had similar values to those of Madison.

For the bed sediment deposit, field investigations on the particle size distribution are not as numerous as the runoff sediment in the literature. One of the available particle size survey is measured in an open drainage system in Malaysia. Bong et al. (2014) introduced a complete procedure to analyze deposits in storm sewers in Malaysia. They found 71% sand (0.05-2 mm), 28% grit (over 2 mm) and 1% silt & clay (under 0.05 mm) in their deposits. The d_{50} of the deposits is 0.6 mm, which is over 10 times that in stormwater runoff samples.

Other studies related to sediment deposits only mentioned d_{50} values, which are shown in Table 2. According to this table, the minimum value of d_{50} is relatively large (0.35 mm) compared to the values in stormwater runoff samples, and the maximum value is up to 1 mm. The median size values are larger in storm sewer inlets when compared to those in storm sewer pipes. This is mainly due to sediment capture capacity of storm sewer inlet (or catchbasins), and the particle size decreases inside the pipes compared to that in storm sewer inlets.

Table 2. The median size, d_{50} , of deposit sediment found in storm sewer systems

Sample locations	Nation	Weather	d_{50} (μm)	Source
Storm Sewer Inlet	US	Wet	550	Sansalones et al., 1998
Storm Sewer Inlet	GER	Dry	1000	Grottker, 1990
Storm Sewer	JAP	Dry	350	Shimatani et al., 1989
Storm Sewer	KUW	Dry	400	Almedeij et al., 2010

In addition to d_{50} , the particle mode size (the size with the largest percentage in particle size cumulative curve) is also a useful indicator. Almedeij *et al.* (2010) collected and analyzed 25 sediment samples from storm sewer inlets located in five residential areas in Kuwait. By comparing three particle size parameters, the median particle size d_{50} , the mean particle size d_m , and the mode size d_{md} , they found that the sample median and mean particle sizes vary locally within each site and spatially compared to others, while the mode size is invariant for most of the cases. Therefore, they concluded that the mode particle size d_{md} is a more stable robust estimator for sediment sizes reflecting the similarity found in watershed characteristics and should be used in the bed load transport rate formulas (the sediment transport mechanisms will be detailed in later chapters). The main findings and conclusions from the study of Almedeij *et al.* (2010) are supported by a recent study by Bong *et al.* (2014). Thus, the mode size can be a future study topic for sediment size characteristics.

2.2 Storm sewer sediment wash-off load

Various factors can affect sediment wash-off load from impervious land: sediment buildup, rainfall intensity, rainfall energy, runoff rate, sediment sizes, and land surface characteristics (Vaze and Chiew 2004). Urban storm water management is generally designed to control sediment loadings from the drainage area. Quantifying sediment load from urban impervious areas is important to estimate and reduce pollutant loadings and to support the designs of urban storm water BMPs (Brodie 2006; Kang et al. 2006).

Typically, two methods are commonly used to describe sediment load entering storm sewer system. The first is the empirical method which directly correlates sediment wash-off with the rainfall depth, intensity and runoff volume (Egodawatta et al. 2007; Chen and Adams 2006).

The second method is based on detailed physical models which greatly improve the governing factors for sediment wash-off from urban areas. However, the second method requires very detailed site information. In addition, computational cost is high when the governing equations are solved directly using finite-difference numerical schemes, which usually limits the application of such models to only event-based simulation (Bai & Li, 2012).

The empirical equations are used widely and recommended in this thesis. The first version of the empirical equation was proposed by Sartor et al. (1974):

$$W = W_0(1 - e^{-kIt}) \quad (1)$$

where, W is sediment load entering storm sewer systems (ton), W_0 is the initial sediment on urban surface (ton), k is wash-off coefficient (determined by catchment slope, mm^{-1}), I is rainfall intensity (mm/hr), and t is time (hr).

Eq. 1 was modified by Egodawatta et al. (2007) as:

$$F_w = C_F(1 - e^{-kIt}) \quad (2)$$

where, $F_w = W/W_0$ is fraction wash-off, and C_F is capacity factor. C_F primarily varies with rainfall intensity. However, for simplicity three rainfall intensity ranges were identified where variation of C_F can be defined. For the rainfall intensities less than 40 mm/hr, C_F varies linearly from 0 to 0.5. For rainfall intensities from 40 to around 90 mm/hr, C_F is a constant around 0.5. Beyond 90 mm/hr C_F varies between 0.5 and 1. The wash-off coefficient k is an empirical parameter with units (mm^{-1}) and appears to have no direct physical meaning. In urban areas, the value of k may vary with the catchment slope (from 5.6×10^{-4} to 8.0×10^{-4} for 7% to 10% slope). Based on this equation, the amount of sediment entering storm sewer system within certain area can be determined when the surface sediment mass is obtained. Urban surface sediment mass can be calculated by the product of spatial mass density (in ton/ha) and surface area (ha) (typically the spatial mass density is around 3 ton/ha according to Bai & Li, 2012).

2.3 Erosion

When wet weather flow appears in sewers, combined forces of the hydrodynamic lift and drag forces may exceed the restoring force leading to movement of bed particles (Butler et al., 2003). Studies of erosion began with alluvial channels using Shields diagram (Shields, 1936). Shields

diagram defined the threshold of erosion, that is, the upper area over the curve is the erosion zone. This diagram was developed for alluvial channels and is not suitable for sewers since site conditions are significantly different from alluvial channels (i.e., smaller particles, steeper slopes, unsteady intermittent flows, etc.) (Bertrand-Krajewski *et al.*, 1993).

After that study, several researchers have studied the threshold of erosion using critical shear stress or critical velocity equations. Novak and Nalluri (1984) suggested the following equation for the critical velocity:

$$\frac{V_c}{\sqrt{gd_{50}(s-1)}} = 0.5 \left(\frac{d_{50}}{R} \right)^{-0.4} \quad (3)$$

where, V_c is critical mean velocity,

g is acceleration due to gravity,

d_{50} is sediment median diameter,

s is sediment specific gravity,

R is hydraulic radius.

El-Zaemey (1991) conducted experiments for incipient motion of touching grouped particles for sediment sizes ranging from 2.9 mm to 8.4 mm on both smooth and rough rigid beds in a circular flume with a flat bed and obtained the following relationship for critical velocity:

$$\frac{V_c}{\sqrt{gd_{50}(s-1)}} = 0.75 \left(\frac{d_{50}}{R} \right)^{-0.34} \quad (4)$$

Bong *et al.* (2014) concluded that all the erosion equations developed are in the form of:

$$\frac{V_c}{\sqrt{gd_{50}(s-1)}} = a_1 \left(\frac{d_{50}}{R} \right)^{b_1} \quad (5)$$

where, a and b are coefficients.

Many studies about critical erosion equations are summarized in Table 3.

Table 3. Various models in the literature for sewer sediment erosion motion

Fr_c	Expression in terms of d/R	Experiment conditions	Reference
$\frac{V_c}{\sqrt{(s-1)gd_p}} =$	$0.50(d_p / R)^{-0.40}$	Circular, 1.1% slope, D = 0.152 m	Novak and Nalluri, 1975
	$0.92(d_p / R)^{-0.45}$	Circular, 1.17% slope, D = 0.305 m	Ackers, 1984
	$0.75(d_p / R)^{-0.34}$	Circular, 1.7% slope, D = 0.22 m	El-Zaemey, 1991
	$1.00(d_p / R)^{-0.32}$	Circular, 1.0% slope, D = 0.45 m	Ab Ghani, 1993
	$0.72(d_p / R)^{-0.46}$	Circular, 1.3% slope, D = 0.158 m	Safari <i>et al.</i> , 2015

2.4 Transport

In storm sewer systems, sediment particles may experience continuous exchange between suspension, bed and near bed section. Therefore, movement of sediment particles is complicated. During the motion period, flocculation, aggregation and biochemical reactions among particles also happen. In order to classify the movement clearly, two kinds of transport patterns are introduced according to the distinctive sediment fractions: suspended load and bed load transport.

- Suspended load

Suspended load is an important part of sewer solids transport, because it can occupy up to 80-90% of the total mass of solids transported in the sewer system (Ashley *et al.* 1994). And the predominant particles in suspension are about 40 μm (Ashley and Crabtree 1992). Full suspension occurs when the Rouse number (η^*) is less than 3 (Ashley and Verbanck, 1996):

$$\eta^* = w_s / \kappa U^* \quad (6)$$

where, η^* is Rouse number,

w_s is particle settling velocity,

U^* is fluid bed shear velocity,

K is von Karman's constant (around 0.4).

Suspended solids have low settling velocity: 0.6 mm/s for dry weather sewage and 0.2 mm/s for stormwater (Ashley & Verbanch, 1996). Suspended solids concentration profile has a sharp increase near the sediment bed (Schlutter & Schaarup-Jensen, 1998).

- Bed load

Particles rolling, saltation and sliding on the bed are bed load particles. Sediment bedload transport happens under rigid boundary (relatively clean pipe) or loose boundary (pipe with deposited bed) condition. Many experiments were conducted under the rigid boundary condition. Once the flow becomes steady and uniform, the sediment supply rate in the upstream is gradually increased until some permanent deposits appear in the pipe. This is the limit of deposition experimental methodology. Equations that were used to predict bed load transport capacity and developed based on previous method are presented in Table 4. For comparison purposes in this report, alternative equations will be re-arranged to contain only the volumetric sediment concentration C_v and is expressed as a function of the other variables. C_v represents the ratio of sediment volume being transported per unit time and the discharge rate of water, which shows the bed load transport capacity under certain flow rate.

Table 4. Equations for sediment transport over rigid boundary

Authors	Equations	Experimental range of C_v
Macke (1982)	$C_v = \frac{\lambda_0^3 V_s^5}{30.4(s-1)w_s^{1.5}A};$ $w_s = \frac{1000[9\nu^2 + 10^{-9}d_p^2g(s-1)(0.03869 + 0.0248d_p)]^{1/2} - 3\nu}{0.11607 + 0.074405d_p}$	$1.0 \times 10^{-7} \sim 1.7 \times 10^{-3}$
Mayerle et al. (1988)	$C_v^{0.18} = \frac{0.07V_s}{\sqrt{gd_p(s-1)}} D_{gr}^{0.14} \left(\frac{d_p}{R}\right)^{0.56} \lambda_s^{-0.18};$ $D_{gr} = \left(\frac{(s-1)g}{\nu^2}\right)^{1/3} d_p$ $\lambda_s = 1.13\lambda_0^{0.98} C_v^{0.02} D_{gr}^{0.01}$	$2.04 \times 10^{-5} \sim 1.28 \times 10^{-3}$
May (1989)	$C_v = 0.0211 \left(\frac{y_0}{D}\right)^{0.36} \left(\frac{D^2}{A}\right) \left(\frac{d_p}{R}\right)^{0.6} \left(\frac{V_s^2}{g(s-1)D}\right)^{1.5} \left(1 - \frac{V_c}{V_s}\right)^4$	$3 \times 10^{-7} \sim 4.43 \times 10^{-4}$
Ghani (1993)	$C_v^{0.21} = \frac{0.32V_s}{\sqrt{gd(s-1)}} D_{gr}^{0.09} \left(\frac{d_p}{R}\right)^{0.53} \lambda_s^{0.21}$	$1.0 \times 10^{-6} \sim 1.45 \times 10^{-3}$

where, V_s is the self-cleansing velocity (i.e. resulting in transport without deposition);

V_c is the critical erosion velocity;

w_s is particle settling velocity;

s is the particle specific gravity;

A is cross-section flow area;

ν is water kinematic viscosity;

d_p is the particle diameter;

g is gravitational acceleration;

C_v is the volumetric sediment concentration (discharge rate of sediment / discharge rate of water);

D_{gr} is grain diameter in dimensionless term;

R is hydraulic radius;

λ_s is the overall friction factor;

λ_0 is the pipe friction factor;

y_0 is water depth in pipe;

D is pipe diameter.

All parameters are in SI units.

In addition to the rigid boundary situation, various experiments were conducted by transporting sediment over a loose sediment layer. Equations that were developed for this condition are presented in Table 5.

Table 5. Equations for sediment transport over loose boundary

Authors	Equations	Experimental range of C_v
EI-Zaemey (1991)	$C_v^{0.165} = \frac{0.52V_s}{\sqrt{gd_p(s-1)}} \left(\frac{W_b}{y_0}\right)^{0.4} \left(\frac{d_p}{D}\right)^{0.57} \lambda_{sb}^{-0.1}$	$1.1 \times 10^{-5} \sim 5.12 \times 10^{-4}$
Perrusquia (1991)	$C_v = 15.3 \left(\frac{W_b}{D}\right) \left(\frac{y_s}{D}\right)^{-0.7} \left(\frac{D^2}{A}\right) \left(\frac{h}{D}\right)^{0.19} \lambda_b^{2.6}$ $\times \left(\frac{d_p}{D}\right)^{-0.63} D_{gr}^{-0.96} \left(\frac{V_s}{g(s-1)D}\right)^{2.1}$	$3.0 \times 10^{-5} \sim 4.08 \times 10^{-4}$
May (1993)	$C_v = \eta_1 \left(\frac{W_b}{D}\right) \left(\frac{D^2}{A}\right) \left(\frac{\theta \lambda_s V_s^2}{8g(s-1)D}\right)$	$3.9 \times 10^{-6} \sim 1.29 \times 10^{-3}$
Ghani (1993)	$C_v^{0.16} = 0.85 \frac{V_s}{\sqrt{gd_p(s-1)}} \left(\frac{W_b}{y_0}\right)^{0.18} \left(\frac{d_p}{D}\right)^{0.34} \lambda_s^{0.31}$	$2.0 \times 10^{-6} \sim 3.7 \times 10^{-5}$

where,

C_v is the volumetric sediment concentration (discharge rate of sediment / discharge rate of water);

W_b is width of sediment bed;

V_s is the self-cleansing velocity (i.e. resulting in transport without deposition);

d_p is the particle diameter;

s is the particle specific gravity;

y_0 is water depth in pipe;

D is pipe diameter;

λ_{sb} is the deposit friction factor;

y_s is the deposit depth;

A is cross-section flow area;

η_1 is transport coefficient;

h is the depth of water above sediment bed;

θ is pipe tilting angle.

All parameters are in SI units.

Though rigid and loose boundary conditions have different equations, a general relationship can be developed based on the method of Graf and Acaroglu (1968). They theoretically analysed the hydrodynamic forces acting on the sediment particles and developed a sediment transport model by defining two dimensionless parameters: the shear intensity parameter (ψ) and the transport parameter (ϕ), which have the following forms:

$$\psi = \frac{(s-1)d_p}{SR} \quad (7)$$

$$\phi = \frac{C_v R V_s}{\sqrt{(s-1)g d_p^3}} \quad (8)$$

where, S is the energy slope of the flow and all parameters are in SI units. They also proposed a relationship for $\phi \sim \psi$:

$$\phi = 10.39\psi^{-2.52} \quad (9)$$

Many researchers have developed $\phi \sim \psi$ relationship based on their experimental data obtained under rigid or loose boundary conditions, as summarized in Table 6, and good correlations are claimed. Therefore, this type of equations has been frequently seen in recent literature.

Table 6. Sediment transport models developed in the literature based on ϕ and ψ

Expression in terms of ψ	Conditions	Reference
$\phi = 10.39\psi^{-2.52}$	Loose boundary	Graf and Acaroglu, 1968
$\phi = 10.39\psi^{-1.5}(1 - 0.045\psi)^{2.5}$	Loose boundary	Graf and Suszka, 1971
$\phi = 6.30\psi^{-1.80}$	Rigid boundary, D = 0.225 m, 1.1% slope, $C_v < 2400$ ppm	Ojo, 1980
$\phi = 9\psi^{-2.04}$	Rigid boundary, D = 0.305 m, 1.3% slope, $C_v < 2400$ ppm	Novak and Nalluri, 1984
$\phi = 100\psi^{-4.5}$	Rigid boundary	Nalluri, 1992
$\phi = 16.5(\psi_b - 0.036)^{1.67}$	Loose boundary	Ota and Nalluri, 2003
$\phi = 1.84\psi^{-1.45}$	Rigid boundary, D = 0.220 m, 1.7% slope, $C_v < 2000$ ppm	Safari, et al., 2015

where, ψ_b is bed shear intensity parameter ($= \frac{(s-1)d_p}{S^*R}$, S^* is slope of bed deposit).

2.5 Deposition

- Deposit build-up

The process of deposit built up was shown by Butler et al. (2003). At first, when flow velocity or turbulence level decreases, there will be a net reduction in amount of sediment held in suspension. Then, sediment particles accumulate into a stream and transport near the bed. With further reduction of velocity, sediment will form a deposited bed. Finally, sediment transport will cease, when velocity is further reduced (reaching critical deposit velocity).

There are two methods (deposit build-up rate and deposit profile) to describe deposit development. For deposit build-up rate, Ashley & Crabtree (1992) showed that it is possible to predict the deposit build-up rate in small sewers for specific site, whereas estimating the rate in larger sewers is difficult.

For deposit profile, Lange and Wichern (2013) found that the deposit profile will be smoother when the deposition time extends. Also, they showed that significant increases in deposit

profile are associated with rainfall and inflow peaks, which is mainly because of the introduction of sediment from catchment surface.

Bertrand-Krajewski et al. (2006) presented a continuous field experiment during 4 years to monitor deposition accumulation in a 2.0 m diameter egg-shaped combined sewer in Lyon. The deposition depth (measured every 5 m by a metal rod) is an important variable to describe the development of deposit profile. The profile after 24 months shows an increase of both deposit volume and mass. And the mean bottom slope increases progressively and contributes to the equilibrium of deposition and erosion. They concluded that the deposit profile irregularities are associated with sewer element changes such as street inlets, lateral connections and house connections.

A field observation conducted by Laplace et al. (1992) showed that the total deposit volume increased from 0 to 100 m³ in 480 m long sewer during two years. They also concluded that the maximum intensity and the number of dry days preceding the rain can determine the increase of the deposit volume. Further, the development of sediment volume has an asymptotic tendency, which means that as solid transport capacity increases, the size of deposited solids increases and the sediment deposition decreases.

In flumes, there are many rules when bed deposits develop with flow over them. Flow over a loose deposit bed can introduce special features which are a variety of bed forms. Ripples appear at low shear stress, when shear stress progressively developed they can turn into dunes.

After further increase in shear stress, dunes are washed-out and flat beds are formed with increasing flow velocities. However, the same kind of observation in storm sewers is unavailable, which means that more studies should be conducted to study the sediment deposit changes with flow rate

- Clean methods dealing with bed deposits

To maintain the proper sewer function, cleaning is needed. Cleaning can be either scheduled or unscheduled. Scheduled cleaning can remove deposits before the blockage occurs. This preventive cleaning can reduce the risk of serious impacts caused by urban surface flood and huge surcharge flows after heavy storms. Scheduled cleaning needs other information related to frequent blockage to ensure higher efficiency, such as historical record, inspection data, pipe age and material. The unscheduled cleaning as a passive reaction is always related to an emergency event to clear a blockage, restore pipe capacity to full flow, and relieve a surcharging situation in the sewer that has caused a backup into homes or an overflow.

There are several cleaning techniques used to clear blockages and to act as preventative maintenance tools, belonging to three main kinds: hydraulic cleaning, mechanical cleaning and chemical cleaning (UAEPA, 1999).

Hydraulic cleaning

Hydraulic cleaning can be further divided into flushing and high velocity jetting. France and Germany have developed many flushing systems using the concept of “dam break”. In the flushing process, huge amount of water is introduced in sewers and the all of the floating material, some sand and grit are removed. High velocity jetting is provided by high pressure water, which is directed against the wall of sewer. This method can remove debris, grease build-up and roots. There are other devices (balls, kites, bags, scooters, etc.) that can improve the performance of high velocity jetting method (USEPA, 1999).

Mechanical cleaning

Mechanical cleaning methods use equipment to physically remove the material from the walls and invert of the sewer pipe. Mechanical cleaning also can be divided into two parts: rodding machine and bucket machine (USEPA, 1999).

Small engine rodding machines are inexpensive and can provide an efficient way of cleaning in small systems, which is a good supplement of large equipment. Larger mechanical rodding machines are equipped with flexible steel rods and an engine to provide the force to rotate, push, and pull. This kind of machine is available in both truck-mounted and trailer-mounted models and a variety of different engine sizes are available for each type of unit. Some truck-mounted units are more powerful since the vacuum hose can take off all the materials from the sewer system. Some rodding machines also utilize high velocity water instead of steel rods to cut materials from the sewer wall, which can also flush the material out.

A bucket machine is equipped with a set of specialized winches that pull a special bucket through a sewer to collect debris. The captured materials are then physically removed from the sewer. Operating bucket machines is a very labor-intensive process. Therefore, power buckets are normally used only for specific cleaning purposes, especially removing large amounts of debris from larger sewers.

Chemical cleaning

Chemical cleaning is used to control roots, grease, odors (H_2S gas), concrete corrosion, and insects. The effectiveness of a particular chemical largely depends on the exact nature of the problem and site specific circumstances. In most cases, these compounds tend to make this method expensive (Arbour & Kerri, 1997 and USEPA, 1999).

2.6 A collection of experiments on sediment movement in storm sewers

Table 7 summarizes experiments on sediment movement in storm sewers reported in the literature. As can be seen in the table, most studies focused on small pipes (D less than 0.5 m), flat slopes (less than 2%), and relatively small particles (d_{50} less than 8 mm). Although these experiments can describe the sediment movement, the pipe sizes are much smaller than the trunks in typical sewer systems and particles are smaller than the coarse sediment (gravel or winter sanding). The equations developed from these experiments work well in small pipes, for flat slopes and smaller particles; however, their reliability for real world conditions is uncertain and further study is needed.

Table 7. Summary of experiments about sediment movement in storm sewers

Author	Year	Flow conditions		Pipe conditions					Sediment characteristics			
		V (m/s)	Depth ratio (y ₀ /D)	Pipe size (mm)	Pipe length (m)	Pipe material	Slope	Pipe roughness (k)	Sediment size d ₅₀ (mm)	C _v 10 ³ (ppm)	Specific Gravity	Sediment bed thickness (mm)
Novak and Nalluri	1975	-	0.15-0.87	152	10	PVC	0.011	≈ 0	0.6-50	0.02-2.4	1.18-7.8	0
		-	0.15-0.88	305	8	Plexiglas		≈ 0	0.6-50	0.02-2.4	1.18-7.8	0
Ackers	1984	0.5-1.5	0.37-1.0	450	21	PVC	0.013	≈ 0	0.57-7.9	0.05-2.1	2.62-2.65	0
Mayerle et al.	1988	0.38-1.4	0.18-0.79	152	20.5	PVC	0.0084	≈ 0	0.5-8.74	0.02-1.14	2.55	0
EI-Zaemey	1991	0.36-0.9	0.14-0.91	305	12.75	uPVC	0.0117	0-1.4	0.53-8.4	-	2.59-2.61	47-120
Perrusquia	1992	0.49-16	0.07-0.51	225	25	concrete	0.002-0.006	≈ 0	0.9,2.5	0.03-0.408	2.65	45-90
May	1993	0.49-1.1	0.37-1.0	158	21	PVC	0.0135	≈ 0	0.57-7.1	0.05-2.1	2.62-2.65	0
		0.5-1.5	0.37-0.76	300	21	concrete		0.15	0.57-7.11	0.05-2.1	2.62-2.65	0
		0.47-0.73	0.5-1.0	450	21.3	concrete		0.141	0.47-0.73	0.05-2.1	2.63-2.64	1.3-130
Ghani	1993	0.5-1.2	0.2-0.8	305	20.5	PVC	0.006	0-1.34	0.46-8.4	0.001-1.3	2.53	0
		0.5-1.22	0.5-0.76	450	21	concrete	0.01	≈ 0	0.72-8.2	0.002-0.037	2.53-2.59	0.9-103.5
Ota and Nalluri	2003	-	0.18-0.63	225	-	concrete	-	0-0.7	0.6-5.7	0.02-2.4	2.65	0
		-	0.18-0.64	305	-	uPVC	-	0-0.7	0.6-5.8	0.02-2.4	2.65	0
Azamathula et al.	2011	0.35-1.75	-	305	-	Plexiglas	0.005-0.02	1	0.4-1	0.1-0.5	2.0-2.65	0
Safari et al.	2013	-	-	300-460	13.5	PVC	-	≈ 0	0.87-7.72	-	2.65	0
Safari et al.	2015	0.34-0.63	0.15-0.5	220	7.2	Plexiglas	0.017	≈ 0	0.45-6	0.07-2.0	2.65	0

2.7 Pollution potential

It has been widely recognized that storm sewer sediments can pose a potential risk to the receiving water courses for contaminants such as heavy metals, ammonia-nitrogen, phosphorous, and fuel additives *etc.* which can be attached to and transported by the sediment. Previous researches have pointed out the density and the particle size distributions most affect the transport of the solids and associated pollutants (Characklis and Wiesner, 1997). Larger particles in storm water tend to settle out, whereas smaller particles remain suspended in storm water and travel great distances. In addition, smaller particles have a greater specific surface area, allowing more adsorption of dissolved constituents onto the surface of the particles and therefore have a greater contaminant content per unit mass. Vignoles and Herremans (1995) examined the heavy metal associations with different particle sizes in stormwater samples from Toulouse, France. Table 8 shows a relationship between metal distribution and particle size. Majority of metal is attached to sediment less than 100 μm , which means that fine sediment ($<100 \mu\text{m}$) might affect the environment most.

Table 8. Metal distribution in different sizes of particles (Vignoles and Herremans, 1995)

Particle size (μm)	Metal distribution (%)							
	Cadmium	Cobalt	Chromium	Copper	Manganese	Nickel	Lead	Zinc
<10	46	60	71	63	71	63	73	60
10-100	36	31	24	30	21	29	23	35
>100	18	9	5	7	8	8	4	5

2.8 Summary

Storm sewer sediment comes from a number of possible sources: atmospheric deposition, wash-off from the surfaces within the catchment, sewer pipes themselves and construction sites. Due to different sources of sediments, these solids cover a wide size range. There are three classical grain size classifications for sediments including ASTM D 2487, ISO 14688-1, and Wentworth Scales.

Besides, a storm sewer sediment classification method was developed by Roesner and Kidner mainly based on particle sizes. Particle size distributions in stormwater runoff have received significant attention; however, particle size information in sediment deposits in storm sewer pipes or catchbasins is still very limited. Sediment loading is controlled by the initial sediment on urban surface, the catchment slope, the rain intensity, and the rainfall duration. Sediment movement includes three parts: erosion, transport and deposition. In terms of sediment blockage problems, sediment critical erosion velocity and sediment self-cleansing velocity are important parameters. Also, a collection of different experiments about sediment movement in storm sewers is presented. For the pollution potential, since majority of metal is attached to sediment less than 100 μm , the fine sediment might affect the environment most.

Chapter 3: Experimental Study of Hydraulics and Sediment

Capture Efficiency in Catchbasins¹

Catchbasins (also known as gully pot in the UK and Australia) are used to receive surface runoff and drain the stormwater into storm sewers. The recent interest in catchbasins is to improve their effectiveness in removing sediments in stormwater. An experimental study was conducted to examine the hydraulic features and sediment capture efficiency in catchbasins, with and without a bottom sump. A sump basin is found to increase the sediment capture efficiency significantly. The effect of Inlet Control Devices, which are commonly used to control the amount of flow into the downstream storm sewer system, is also studied. These devices will increase the water depth in the catchbasin and increase the sediment capture efficiency.

3.1 Introduction

Stormwater sediments can cause many negative impacts on the receiving water bodies. High levels of sediment concentration contribute to higher turbidity which limits sunlight penetration thereby prohibiting the growth of aquatic plants (Aryal and Lee, 2009). Sedimentation also can clog fish spawning grounds and reduce the conveyance capability of the streams or rivers receiving water from storm sewer system. Additionally, pollutants adhering to sediment, including heavy metals, salt, hydrocarbons and high concentration of nutrients (e.g., Total Nitrogen and Total Phosphorus), pose direct threats to aquatic life and water quality (City of Calgary, 2011; USEPA, 1993). In order to remove sediment, various sediment control practices have been adopted recently (Wilson et al., 2009, He and Marsalek, 2014). Catchbasins receive surface runoff and can potentially retain

¹ A paper based on this chapter has been submitted to Water Science and Technology.

sediment, grit and detritus on catchbasin bottom before these are flushed into the storm sewers (Aronson et al., 1983). Thus, the study on sediment capture efficiency in catchbasins is important.

A number of factors impact on the sediment capture efficiency in catchbasins. The most important factor is probably the sediment characteristics. Generally, sediment entering catchbasins is non-cohesive, with an average specific gravity of 2.65 (Clegg et al., 1992) for reasonably large particles. Inflow sediment concentrations also affect the sediment capture efficiency. The sediment size is the key variable to determine sediment settling ability. The particle median size d_{50} is usually treated as the characteristic size of a group of particles. Typically, sediment found in storm sewer systems can be divided into three kinds: suspended sediment, bedload sediment and bed deposit sediment. The sizes of suspended sediment vary from less than 1 μm to over 600 μm with a value of d_{50} between 8 μm and 100 μm (Selbig and Bannerman, 2011; City of Calgary, 2011; Goncalves and Van Seters, 2012; Boogaard et al., 2014). Bed deposit sediments are characterized by bigger sediment sizes. Several studies were found with a storm sewer deposit d_{50} value varying between 0.25 mm and 1 mm (Grottker, 1990; Sansalone et al., 1998; Almedeij et al., 2010; Bong et al., 2014). The bedload sediment size is believed to be between the sizes of the previous two classes. In northern climates, large particles such as gravel as large as 5 mm are used for winter de-icing the roads and, since some of these particles can be flushed into the catchbasin, such gravel could be an important sediment source. While these larger particles may only contribute a part of the overall sediment load, their presence can lead to significant blockages in the receiving storm sewer system if they are not captured prior.

The earliest research about the sediment capture efficiency of catchbasins was conducted by Lager (1977). Lager measured the sediment capture efficiency under laboratory conditions for various

scenarios (i.e., flow rates ranging from 7 to 178 L/s, particle sizes from 0.1 to 2 mm and with d_{50} values concentrated around 0.3 mm and 0.8 mm, and various catchbasin designs, albeit all with sumps). With respect to the sediment capture efficiency, it was found that catchbasins can remove medium to coarse sands very efficiently over a wide range of flow rates (i.e., the capture efficiency can reach 65 to 90%). At the maximum flow rate, the capture efficiency can still reach 35%. However, a negative capture efficiency may appear when the sediment deposition in a catchbasin is over 40 to 50% of the sump depth which is mainly caused by scour. Although they observed the sediment capture efficiency in specific catchbasins with various designs, they did not produce a general prediction method. Aronson (1983) collected field data to evaluate the performance of catchbasins in controlling pollution. More than 40 sites were investigated showing 60 to 97% capture efficiencies for Total Suspended Solids. However, this study focused more on the removal of chemical substances. In 1995, Butler and Karunaratne studied solids trap efficiency in a roadside gully pot and reported capture efficiencies ranging from 15% to 95%.

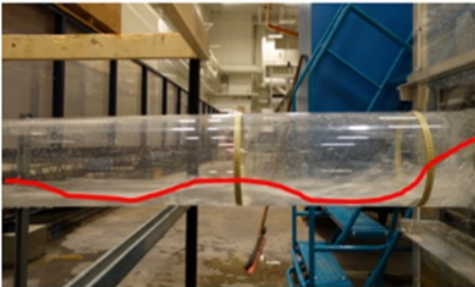
Wilson et al. (2009) introduced the use of the Péclet number (expressed as a ratio of convective particle transport by settling to transport by turbulent diffusion) from reservoirs to stormwater treatment facilities including catchbasins and “standard sumps” (a cylindrical tank with a vertical axis connecting two horizontal pipes). This work provided a fundamental approach to predict the sediment capture efficiency. Howard et al. (2012) measured the sediment capture efficiency of several standard sumps under laboratory conditions and successfully developed an equation to predict the sediment capture efficiency based on the methods from Wilson et al. (2009). Standard sumps are similar to catchbasins, thus, their analytical method can be partly adapted for the analysis of sediment removal in catchbasins.

The configuration design of catchbasins also affects the flow hydraulics and sediment capture efficiency. Municipalities typically have their own design guidelines. In Calgary, Canada, catchbasins do not have sumps (City of Calgary, 2011). In the 1940s and 1950s, from City of Calgary's point of view catchbasin sump cleaning and maintenance required too much effort. Hence sumps were removed from design practice while existing sumps were filled in. In addition, since the late 1980s, the drainage systems in new subdivisions in Calgary have been designed based on the dual drainage principle. As part of Calgary's design practice, Inlet Control Devices (ICDs, see Figure 4) are typically installed in catchbasins to control the amount of the flow into the downstream pipes to reduce the potential of the storm sewer system getting overloaded during severe storm events. An ICD is usually a steel plate with a small opening, installed at the entrance to the storm sewer, to control the amount of the flow to be released to the storm sewer system (City of Calgary, 2011).

3.2 Methods

Experiments of a full-size catchbasin configuration were conducted in the T. Blench Hydraulic Laboratory at the University of Alberta. The setup, from upstream to downstream, consisted of a sand & water feeding system, catchbasin and outlet pipe (see Figure 3). Water was supplied by a pump, and the flow rate was measured using a magnetic flow meter with a test range from 5 to 28 L/s. Though this range was relatively small due to the experimental constraints, a wide range of flow conditions can be simulated by using particles of various settling velocities (0.002 to 0.17 m/s, see Table 9). Combined with a general analysis, it is possible to predict the flow and sediment behavior under a large flow rate. A sand feeder (Vibra Screw Inc., Model SCR-20) was used to control the sand feeding rate (g/s) by adjusting its rotational speed (rpm). Sand was added into the water flow through an opening on the crown of the inlet pipe, which had a diameter of 150 mm.

At the end of the inlet pipe, a 90° elbow was installed to force the water flow to impinge onto the center of the catchbasin. The use of the elbow for the inflow will likely result in a larger inflow velocity compared to the actual catchbasin; however, our preliminary tests showed that this has negligible effect on sediment removal efficiency. The catchbasin was 0.9 m square and 1.8 m deep. A false bottom could be added in the catchbasin to represent a catchbasin without a bottom sump. The outlet pipe was a 250 mm diameter Plexiglas pipe. At the entrance of the outlet pipe, an ICD could be installed. The ICD (see Figure 4) was a steel plate with a small opening to control the amount of the flow to be released downstream. The opening of the ICDs consisted of one circular hole and one rectangular area. The circular size of ICD was denoted by its center hole diameter (D). Three opening sizes of $D = 50, 70$ and 100 mm were studied in this paper (ICD D50, D70, and D100).



7 L/s without sump and with ICD 100

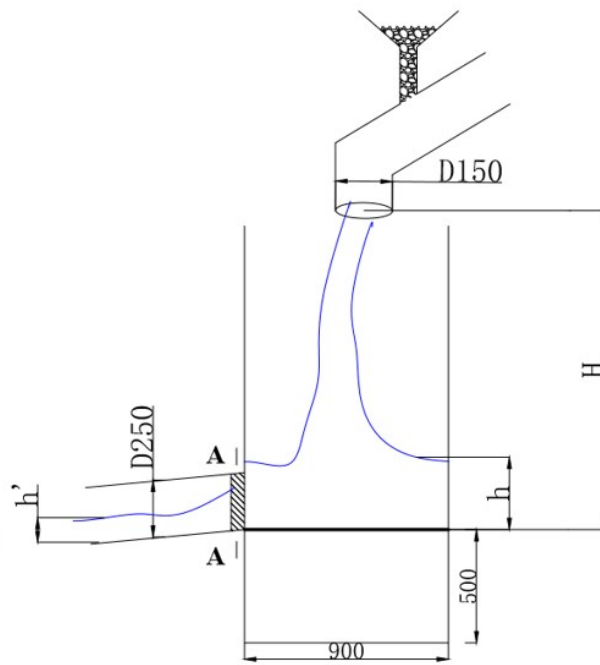


Figure 3. Experimental setup and flow observations

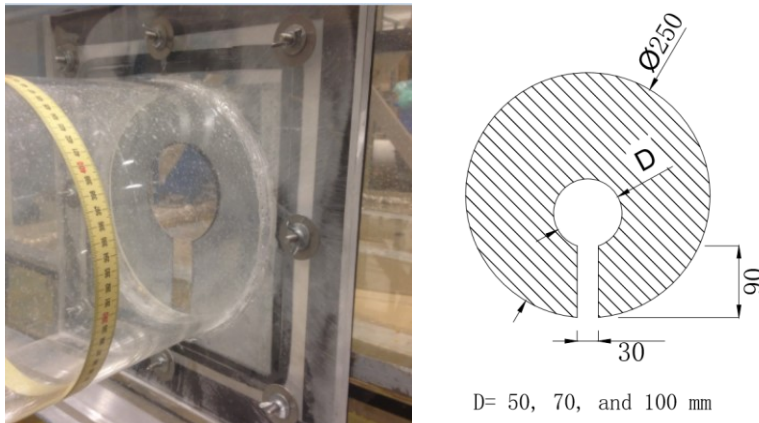


Figure 4. An ICD installed in the outlet pipe, and ICD dimensions

Six size groups of sediment were used in the tests (see Table 9 for detailed information). The finest sediment used was BT-13 glass beads (Manus Abrasive System Inc.) with a d_{50} of $62 \mu\text{m}$. The $100 \mu\text{m}$ size group sand was sieved to be between 75 and $150 \mu\text{m}$, and $200 \mu\text{m}$ size group sand was sieved to be between 150 and $250 \mu\text{m}$. Relatively coarse sands Sil 4 ($d_{50} = 250 \mu\text{m}$), Sil 7 ($d_{50} = 450 \mu\text{m}$) and Sil 8/16 ($d_{50} = 1800 \mu\text{m}$) (Sil Industrial Minerals Inc.) were also used in the experiments. Sil 4, Sil 7, and Sil 8/16 sand are relatively uniform, since their uniformity coefficients ($C_u = d_{60}/d_{10}$, Yalkowsky & Bolton in 1990) are calculated as 1.9, 2.2, and 2.6. A total of six size groups provide a relatively large sand size range for this study. All sands had a 2.65 specific gravity and the glass beads have a 2.51 specific gravity.

Table 9. Sand information

Sand type	Size range (μm)	d_{50} (μm)	Cu	w_s (cm/s)	Picture
BT-13	44-88	62	N/A	0.18	
100 μm	75-150	100	N/A	0.47	
200 μm	150-250	200	N/A	1.71	
Sil 4	40-1000	250	1.9	2.50	
Sil 7	40-1000	400	2.2	5.61	
Sil 8/16	40-2400	1800	2.6	16.65	

Three catchbasin scenarios were studied: (1) without sump and without an ICD (named “Without Sump”); (2) without sump and with an ICD (named “With ICD”); and (3) with a sump (50 cm depth) and without an ICD (named “With Sump”). In each scenario, the test procedures were the same. The test procedures followed a standard method for estimating removal efficiency of sumps and hydrodynamic separators (ASTM International, 2012). The first step was to run water until steady state conditions set in and record the relevant hydraulic parameters including the water flow rate, water depth in the inlet pipe (by a tape ruler), water depth in the catchbasin, and the water depth in the outlet pipe (based on photos). Then, the sand adding rate was determined to limit the sand concentration to be less than 0.15 mg/L, a value reported as the normal suspended sediment concentration in storm sewers (Ab Ghani, 1993). Since this study only focuses on pure sediment

settling without the scour of a previously deposited sediment layer, the chosen small concentration was only able to form a thin sand bed deposited on the catchbasin bottom. Subsequently, the sand feeder was set by adjusting the rotational speed to obtain the required sand feeding rate. The feeder was run for 5 minutes for each experiment. Tests with a 10-minute duration were also conducted which showed a difference of less than 5 %. After each test, the sediment captured at the bottom of the catchbasin was collected, dried and weighed. The capture efficiency of the catchbasin was obtained from the ratio of the amount of captured sand to the amount of sand added. The test flow rates were 5, 7, 14, 21, and 28 L/s, and six types of sand were tested for each flow rate. Experiment parameters are summarized in Table 10.

Table 10. Experiment parameters for sediment removal efficiency in catchbasin

Parameters	Range	Note
Water flow rate (L/s)	5, 7, 14, 21, and 28	This range is a typical range found in stormwater management and design manual.
Sediment particle sizes D₅₀ (mm)	62, 100, 200, 250, 450, and 1800 μm	Except for the last one, particles are uniformly graded.
Sediment flux (g/s)	10.5, 21, 31.5, and 42	These values represent a sand volume concentration of 0.1%.
Sump	With/without	Test how much these structures can affect sediment removal efficiency. And find out the optimized sediment control structure.
ICD	With ICD (test 50, 70, and 100 diameters circular opening); Without ICD	Values are obtained from stormwater management and design manual.

3.3 Hydraulics of the flow in the catchbasin

In general, two types of flow conditions can be distinguished in this experiment. For the “Without Sump” and “With Sump” scenarios, the flow in the outlet pipe was relatively tranquil even at the largest flow rate (28 L/s). For the “With ICDs” scenario, the flow in the outlet pipe appeared to be wavy and could not attain a tranquil flow state because of the high speed outflow through the ICD, even for the combination of a small flow rate (7 L/s) and the largest ICD (ICD D100) (see Figure 3). The water depth measurements were recorded by a camera. The water depth above the outlet pipe bottom in the catchbasin for the “Without Sump” and “With Sump” scenarios increased from about 10 cm to 24 cm as the flow rate increased from 5 L/s to 28 L/s. The two sets of depths were quite close at the same discharge rate (see Figure 5). This indicates that the configuration of the outlet structure governed the water depth in the catchbasin rather than the presence of a sump.

The water depth in the catchbasin for the “With ICD” scenario was significantly different from the previous two scenarios: as to be expected, with an ICD, the water level rose quickly with the flow rate. The outflow from the catchbasin corresponded to orifice flow conditions, rather than the open channel flow condition as in the previous scenarios. In particular, with an ICD D50, the water level reached a height of about 90 cm for a relatively small water discharge of 14 L/s.

For orifice flows, the discharge Q can be expressed as:

$$Q = C_d A' \sqrt{2gy} \quad (10)$$

where, y is the water depth above the center of the orifice, A' is the orifice area, and C_d is the discharge coefficient. To simplify the analysis, we treat the ICD as the combination of a circular orifice (with a diameter D) and a rectangular orifice (with a width a , and a height b), see Fig. 4.

Thus, when the water surface position in the catchbasin is about 20% above the opening (Reader-Harris, 2015), the discharge Q can be estimated as:

$$Q = C_d \left[\frac{1}{4} \pi D^2 \sqrt{2g(h - b - 0.5D)} + ab \sqrt{2g(h - 0.5b)} \right] \quad (11)$$

where, the depth of water in the catchbasin above the invert of the outlet pipe is h , the depth to the center of the circular orifice is $(h - b - 0.5D)$ and that to the rectangular orifice is $(h - 0.5b)$.

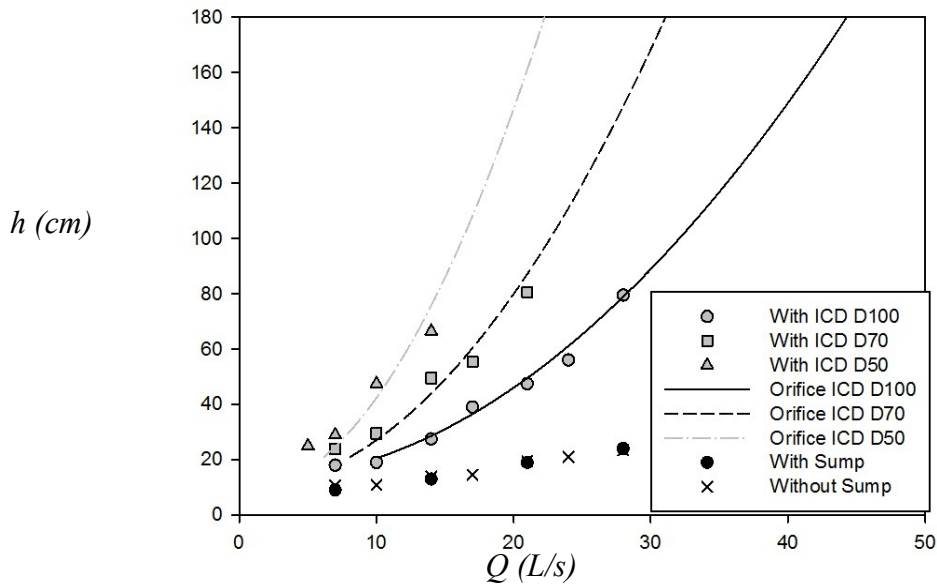


Figure 5. Measured water depth and discharge relation in catchbasins (lines are the fitted orifice equations)

For the ICDs, $a = 3$ cm, $b = 9$ cm, and $D = 50, 70,$ and 100 mm for ICD D50, D70, and D100, respectively. The measured results in Figure 5 are then used to fit a discharge coefficient C_d . $C_d = 0.82, 0.82,$ and 0.73 for ICD D50, D70, and D100, respectively. It is clear that the discharge coefficient C_d is consistently larger than the C_d value of about 0.61 for an idealized orifice (Reader-Harris, 2015). Given the complicated nature of the flow in the catchbasin and our simplified model, the orifice type of equations work quite well and can be used for design purposes.

The energy loss caused by a catchbasin and the water drop can be calculated from the energy difference between the inlet section and the outlet section as follows (see Figure 3 for notations):

$$\Delta H = (H - h') + \left(\frac{V_{in}^2}{2g} - \frac{V_{out}^2}{2g} \right) \quad (12)$$

where, H is the height of the inlet from the datum at the invert of the outlet pipe (see Figure 3), h' is the water depth in the outlet pipe, V is the mean flow velocity, and ΔH is the head loss between the two sections. The subscripts “in” and “out” refer to the inlet and outlet sections of the structure. The relative energy loss (η_E) can be calculated by:

$$\eta_E = \Delta H / \left(H + \frac{V_{in}^2}{2g} \right) \quad (13)$$

The energy loss results are shown in Figure 6. The relative energy loss is quite high, mostly over 60%. It decreases as the discharge increases.

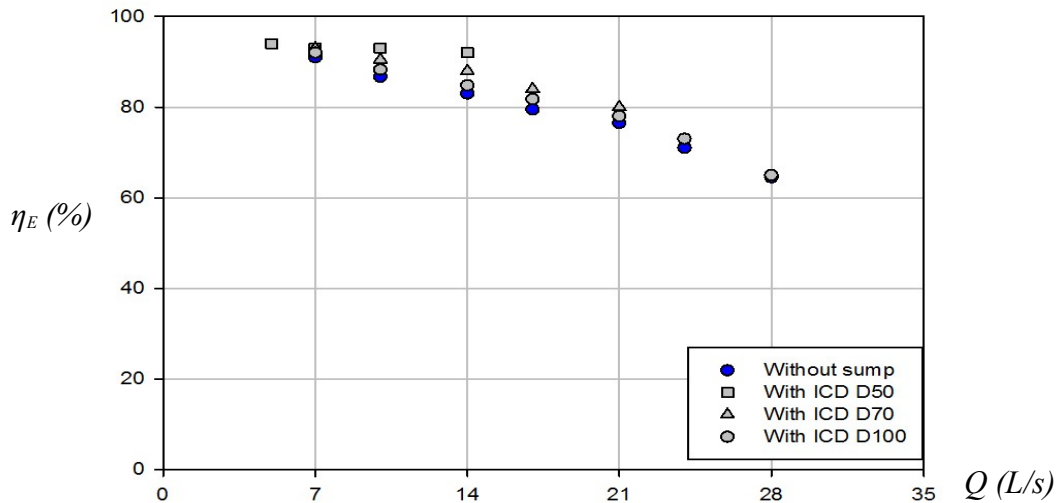


Figure 6. Energy dissipation rate in catchbasins

3.4 Sediment capture efficiency

Ferguson and Church (2004) provided an equation for calculating particle settling velocity (w_s):

$$W_S = \frac{(\rho_P - \rho_W)gd^2/\rho_W}{C_1\nu + (0.75C_2(\rho_P - \rho_W)gd^3/\rho_W)^{0.5}} \quad (14)$$

where, $C_1 = 18$ and $C_2 = 1.0$ for particles in this study; ν is kinematic viscosity (at 20 °C measured in laboratory); d is particle size, usually using d_{50} ; ρ_P is particle density; and ρ_W is water density. Based on the different d_{50} values used in the experiments, the calculated sediment settling velocity is 0.18, 0.47, 1.71, 2.50, 5.61, and 16.56 cm/s, respectively, for the six types of sands, from fine to coarse (see Table 9).

For the “Without Sump” scenario (see Figure 7a), most of the larger particles can be captured at smaller flow rates. The sediment capture efficiency is high for large particles (i.e., over 1 mm in size) for the catchbasin without a sump when flow rate less than 14 L/s. This is mainly caused by the low flow velocity which is hard to transport sediment. When flow rate is increased, the sediment capture efficiency decreases significantly. For example, the capture efficiency for the particles of $d_{50} = 1800 \mu\text{m}$ is over 95% for a flow rate less than 14 L/s. This is mainly caused by the particles’ large settling velocity. However, when the flow rate increases, the increased velocity in the catchbasin will carry more particles out of the catchbasin, and the capture efficiency drops to about 48% at a discharge of 28 L/s. For the sands of $d_{50} = 400 \mu\text{m}$, the capture efficiency decreases from over 83% to less than 28% over the same flow range. The capture efficiency for 200 μm d_{50} sand decrease from 48% to 22% over this flow range, and for the 100 μm d_{50} sand, it decreases from 33% to 18%. For 62 μm d_{50} glass beads, the capture efficiency decreases from 24% to less than 10% and does not vary much with the flow rate.

The sediment capture efficiency for the “With Sump” scenario is shown in Figure 7b. In general, for smaller flow rates the sediment capture efficiency for all six size groups is similar to the case

of “Without Sump”. However, the capture efficiency does not decrease when the flow rate increases, as these particles are settled into the sump. Once settled, it is difficult to re-suspend these particles in the test flow rate range. For example, the capture efficiency for the sand of $d_{50} = 1800$ μm remains high at 95% over the entire flow range. For sand with 250 μm d_{50} , the effect of the sump is noticeable at large flow rate (28 L/s) where the capture efficiency increases from 24% to 64%. But when the particles are small, the effect of the sump is limited.

With an ICD, the water depth in the catchbasin increases. A deep water pool in the catchbasin helps in settling the particles. The results of the sediment capture efficiency with an ICD D100 are shown in Figure 7c. It can be seen that the ICD had no impact on the sediment capture efficiency for the 62 μm d_{50} glass beads (i.e., see the similar curves in Figures 7a and 7c). For sands having a 100 μm and 200 μm d_{50} , the presence of the ICD slightly increases the sediment capture efficiency. For sands with over a 250 μm d_{50} , the sediment capture efficiency slightly decreased for a flow rate less than 15 L/s and then moderately improved compared to the “Without Sump” scenario.

In general, the most important factor influencing the sediment capture efficiency is the sediment size or settling velocity. Small sands (62 μm d_{50} glass beads, 100 μm and 200 μm d_{50} sand) display small sediment capture efficiencies and can be relatively easily flushed out of any catchbasin, even at a very low discharge rate. 400 μm and 250 μm d_{50} sands have moderate sediment capture efficiencies but display a relatively large sediment capture efficiency variation (i.e., over 60%) when the discharge changes. 1800 μm d_{50} sand is relatively hard to be flushed out, hence has the largest retention efficiency. The addition of a catchbasin sump or ICDs has similar beneficial

effects on the sediment capture efficiency because of the increased water depth compared to the “Without Sump” scenario. However, a sump is more effective than the provision of ICDs.

3.5 Model for predicting sediment capture efficiency

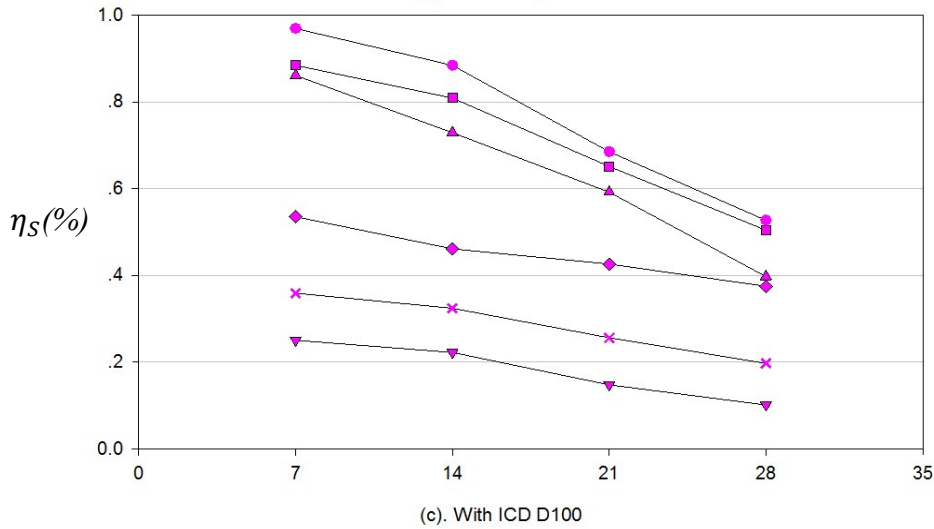
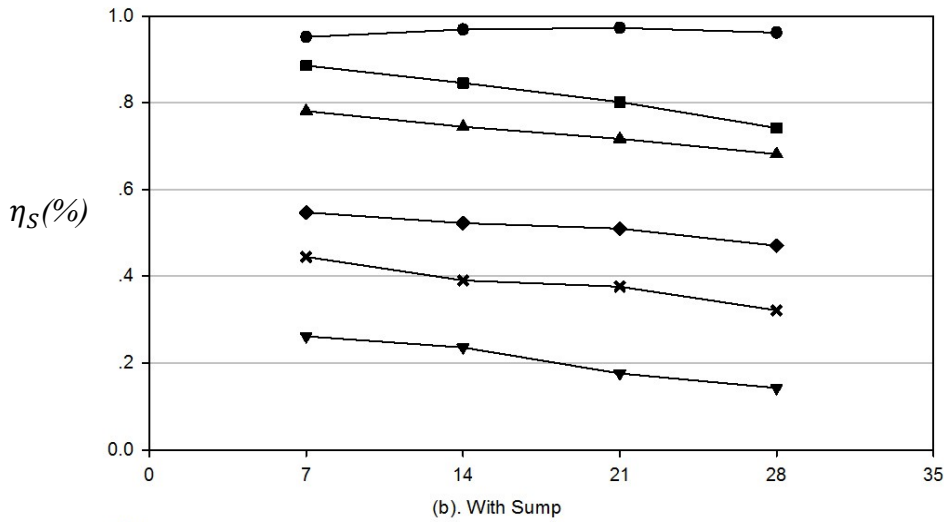
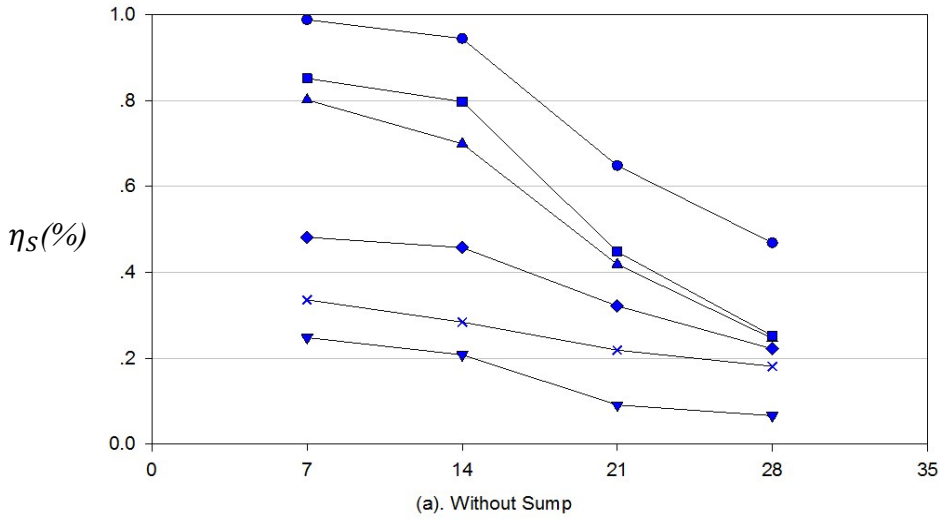
Wilson et al. (2009) proposed an equation for predicting the sediment capture efficiency in hydrodynamic separators (see Eq. 15), which is a function of the Péclet number ($P = w_s l W / Q$, the ratio of the particle settling velocity and the mean flow velocity in horizontal direction, where l is the water depth from water surface to structure bottom in the sump and W is the sump width) and some coefficients (a_2 & b_2).

$$\eta_S = \left[1 + \frac{1}{(a_2 P)^{b_2}} \right]^{-1/b_2} \quad (15)$$

Howard et al. (2011) studied the sediment capture efficiency in storm sewer sumps and incorporated the inflow jet Froude number into the equation, as follows:

$$\eta_S = \left[1 + \frac{1}{(a_3 P / F_j^2)^{b_3}} \right]^{-1/b_3} \quad (16)$$

where, F_j is inflow jet Froude number ($F_j^2 = \frac{V_{in}^2}{g D_{in}}$), D_{in} is inlet jet diameter, and a , b are coefficients.



Q (L/s)

Figure 7. Sediment capture efficiency for different types of sand (the particle d_{50} decrease from the top to the bottom: ●-1800 μm, ■-400 μm, ▲-250 μm, ◆-200 μm, ✕-100 μm, ▼-62 μm

Eq. 15 of Wilson et al. (2009) correlates the sediment capture efficiency as a sole function of Péclet number. Eq. 16 of Howard et al. (2011) also incorporates the inlet jet Froude number to the Péclet number. However, it is believed that sediment traveling distance and settling time are also important parameters for sediment capture efficiency. In this study, a dimensionless traveling distance (l/D_{out}) is also incorporated into Eq. 17. As standard catchbasins do not have a well-defined inlet pipe, use of the inflow jet Froude number is avoided in this study. Note that the mean flow direction in catchbasins is in a downwards direction which is different from the horizontal mean flow in storm sewer sumps. Therefore, the Péclet number P is restated as $\frac{v_s}{V_V}$, where, $V_V (= Q/WW)$ is the vertical mean velocity in the catchbasin. As a result, the proposed equation is:

$$\eta_S = \left[1 + \frac{1}{(a_4 P \frac{D_{out}}{l})^{b_4}}\right]^{-1/b_4} \quad (17)$$

According to Eq. 17, the term PD_{out}/l can be expressed as $v_s D_{out}/V_V l$. V_V and l are functions of Q . Thus, in a catchbasin with a constant W , the sediment capture efficiency is a function of the flow rate, settling velocity and outlet diameter (Q, v_s, D_{out}). Notice that the selection of D_{out} as a length scale is somewhat arbitrary. More studies will be needed to develop a general form of the equation. In general, larger flow rates will result in a lower sediment capture efficiency since the larger flow rate reduces the sediment residence time. By contrast, larger settling velocities and larger outlet diameters will lead to higher sediment capture efficiencies.

The experimental data of the “With Sump”, “Without Sump”, “With ICDs” scenarios as well as other scenarios from the literature (Lager et al., 1977; Howard et al., 2012; Ma and Zhu, 2014) are plotted in Figure 8, with η_S on the vertical axis and PD_{out}/l on the horizontal axis. When PD_{out}/l approaches positive infinity, the capture efficiency can approach 100%. When the range of PD_{out}/l

varies from 0.01 to 10, it represents large variations in flow rates (7 – 178 L/s), water levels (0.1 – 1.8 m), and particle sizes (62 μm - 1.8 mm). Reflecting this considerable parameter range, it is believed that this model can be applied to represent a wide range of design conditions.

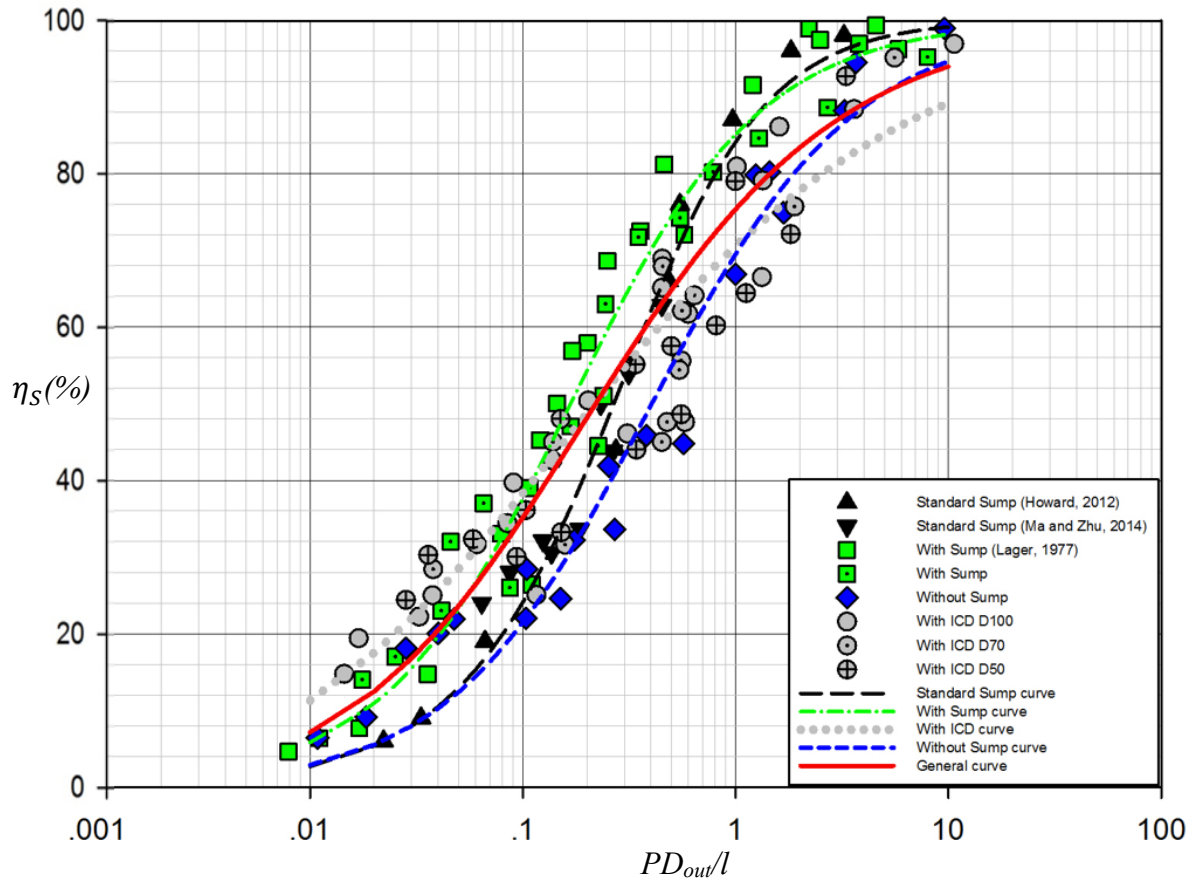


Figure 8. Measured and simulated sediment capture efficiency in catchbasins

Figure 8 illustrates that the fitted curves of the experimental data have similar trends even for different set-ups. The different symbols represent the various structures tested; specifically, the triangle, square, diamond, and circle symbols represent the “storm sewer standard sump”, “catchbasin with sump”, “catchbasin without sump”, and “catchbasin with ICD” scenarios, respectively. For all curves, the sediment capture efficiencies increase from about 0 to over 92% covering the entire test range. The gradient of the change in the sediment capture efficiency varies from small to large and finally returns to small, which represents that the sediment capture

efficiency is relatively stable at very small or large values of flow rates, settling velocities and outlet diameters but changes rapidly between them. For example, in the case of the “catchbasin with sump” scenario, for coarse sand ($d_{50}=1$ mm), the sediment capture efficiency changes from 50% to 99% (49% difference), when the flow rate changes from 178 to 7 L/s. For fine sand ($d_{50}=0.1$ mm), the sediment capture efficiency only has a 44% difference, during the whole flow rate range. However, for the medium size sand ($d_{50}=0.4$ mm), the change is from 15% to 97% (82% difference) for the same flow rate variation.

A general curve for all cases is shown as a solid line. This curve has a $R^2 = 0.85$ and a 10% root mean square error (*RMSE*), which has relatively good fitting and can generally describe the sediment capture efficiency change among different conditions. Although this curve might not be able to predict sediment capture efficiency precisely among specific configurations, it reflects the sediment capture efficiency patterns in all catchbasins. Thus it can provide an approximate sediment capture efficiency for newly planned catchbasins regardless of its configurations. The four curves represent the sediment capture efficiency for the four different scenarios displayed. For the “storm sewer standard sump” (Howard et al., 2012; Ma and Zhu, 2014), “catchbasin with sump” (Lager et al., 1977; current study data), and “catchbasin without sump scenarios” (current study data), the correlation coefficient R^2 value is over 0.96 while the root mean square error (*RSME*) value is less than 6%. This confirms that the newly developed expression of Eq. 17 works well to represent these scenarios. However, for the “catchbasins with ICD” scenario, while the curve still displays a similar pattern, it is not quite as accurate (with 7% *RMSE* and $R^2=0.87$). This might be caused by the D_{out} value (D_{out} is chosen as being equal to the diameter of the ICD circular hole), since the ICD is in fact not composed of solely a circular hole but a combination of

rectangular and circular hole instead. A summary of these curves (equation, $RMSE$, and R^2) is summarized in Table 11.

Table 11. A summary of sediment capture efficiency curves (including equation, $RMSE$, and R^2)

Curve type	Equation	$RMSE$	R^2
General	$\eta_S = \left[1 + \frac{1}{(9.23P \frac{D_{out}}{l})^{0.69}}\right]^{-1/0.69}$	10%	0.85
Standard Sump	$\eta_S = \left[1 + \frac{1}{(2.72P \frac{D_{out}}{l})^{1.34}}\right]^{-1/1.34}$	4%	0.98
With Sump	$\eta_S = \left[1 + \frac{1}{(6.23P \frac{D_{out}}{l})^{0.97}}\right]^{-1/0.97}$	5%	0.96
Without Sump	$\eta_S = \left[1 + \frac{1}{(3.02P \frac{D_{out}}{l})^{0.88}}\right]^{-1/0.88}$	6%	0.96
With ICD	$\eta_S = \left[1 + \frac{1}{(24.73P \frac{D_{out}}{l})^{0.51}}\right]^{-1/0.51}$	7%	0.87

3.6 Summary

In this experiment, the hydraulics and sediment capture efficiency are studied for three different catchbasin structures: “Without Sump”, “With Sump”, and “With ICD”. With respect to the hydraulic features, compared to a catchbasin without a sump, a sump neither changes the water depth in the catchbasin relative to the invert of the outlet pipe nor changes the water depth in the outlet pipe. However, the presence of ICDs increases the water depth significantly. Orifice-type equations represent the “With ICD” scenario appropriately and can therefore be used for design purposes. As to energy dissipation, the amount of dissipation decreases with increasing discharge rate. However, given that it is over 60% in all cases, the energy dissipation is relatively high.

About sediment capture efficiency, as to be expected, it decreases as the discharge rate increases, and is greatest for coarser sediments. 1800 μm d_{50} sand is easily captured. Sands of 250 μm and 400 μm d_{50} both have an over 60% decrease in the sediment capture efficiency, when the discharge increases from 7 to 28 L/s. Smaller particles of 62 μm d_{50} glass beads, 100 μm and 200 μm d_{50} sands are easier to be flushed out of any catchbasin, even at low discharge rates. The presence of a sump improves the sediment capture efficiency, especially for larger particles. The presence of ICDs has a minor influence on the sediment capture efficiency for the smaller particles (62 μm d_{50} glass beads, 100 μm and 200 μm d_{50} sands) at small discharge rates. When the discharge rate is more than 20 L/s, the sediment capture efficiency for all type of sands improves when catchbasin are equipped with an ICD.

A new general expression was developed for predicting sediment capture efficiencies, adapted from previous studies (Wilson et al., 2009; Howard et al., 2012). This expression was used to generate four separate functions reflecting the three scenarios examined as well as the earlier studies, all of which have relatively high correlation coefficients and small *RMSE*. The new expression can be applied for a wide range of flow rates, water levels and particle sizes. In general, the new expression is clear and simple since it only requires direct physical parameters including W , Q , l , D_{out} and w_s , thus making it quite convenient to be applied in urban drainage design.

The proposed equation appears to work well for the data obtained in this study as well as previous data as shown in Figure 8. However, using a simple Péclet along with a simple dimensionless travel distance will likely over-simplify the complicated sediment transport and sedimentation in various types of catchbasins and sumps. It is expected that the turbulence levels in these structures are likely to be very much geometry and flow dependent. In addition, various sediment size

distributions and concentration will also affect the results. Future studies will need to be carried out to test high sediment concentrations (as in major storm scenarios) since the sand concentration is relatively low in this study. Also the effects of sediment composition, cohesive and non-cohesive sediment, as well as sediment deposition need to be studied. Large flow rate and different catchbasin geometry should also be tested in future. Also note seasonal water temperature difference might also result in a sediment capture efficiency.

Chapter 4: Experimental Study of Sediment Movement in a Submerged Pipe on Steep Slopes

In Canada, the last storm sewer pipes (outlets) leading to stormwater ponds are typically steep slope (2%) and submerged in order to avoid odor and winter icing problems. When upstream runoff approached the submerged steep pipes, the flow rate and turbulent level can be reduced which contributes to the deposition. Thus, the sediment movement in a submerged pipe was investigated in an experimental study to understand the detailed deposition processes. Two series of experiments were conducted, including single particle traveling velocity and sediment deposition development. Based this study, the particle traveling velocity is a function of mean velocity, particle size, and pipe slope. The sediment development usually occurred when flow velocity is less than the particle erosion velocity, and the sediment deposition rate can be approximately calculated through the experiment data.

4.1 Introduction

In recent years, sediment depositions in sewer systems have received significant attention. Sediment deposition in sewers reduces flow area and can cause pipe blockage, consequently leading to surcharge flows and urban flood (Butler & Davies, 2011). Thus, there have been many lab and field studies about sediment movement in sewer pipes, in order to solve sediment deposition problems (Ab Ghani, 1993; Perrusquía, 1991; Ota and Perrusquía, 2013; Lange and Wichern, 2013). However, most studies did not pay much attention to system outlets (submerged pipe connecting downstream stormwater pond and upstream manhole). Submerged pipes have significant amounts of sediment deposition. Thus, in order to reduce the amount of deposition, the sediment movement in submerged pipes should be well understood.

As long ago as the mid 1970's and early 1980's several experiment studies, intended to solve the problem of sediment deposition development in sewers, were undertaken around the world (Perrusquía, 1991). The main focus of this stage was to obtain the bed deposition form dimensions. The available methods for predicting the dimensions of bed deposition were transformed from river sediment studies. The distinction for the deposition forms was between ripples and dunes. A method produced by van Rijn (1984) was able to predict the bed deposition height and length. Van Rijn analyzed 84 flumes and field data thus concluding the bed deposition height is a function of particle diameter (d_{50}), flow depth, and a transport parameter. However, these methods were just suitable for wide alluvial channels. The deposition dimension prediction in pipes is still unclear, which becomes one interest driving this experimental study.

In the 1990's, attention focused on the sediment movement in laboratory experiments and complicated city sewer systems. The sediment movement can be generally divided into erosion, transport and deposition. El-Zaemey (1991) conducted experiments on incipient motion of touching grouped particles for sediment sizes ranging from 2.9 mm to 8.4 mm on both smooth and rough rigid beds in a circular flume with a flat bed and obtained a relationship for critical velocity. Erosion processes also play an important role in other design concepts, because an efficient self-cleansing sewer is defined as one maintaining a balance between the amounts of deposition and erosion (Butler et al., 2003). Thus, various methods were suggested for the design of self-cleansing sewers at this stage. In general, the erosion study is relatively mature during decade years of studies. As for sediment transport study, the suspended load transport is not an issue for urban floor/sewer blockage problems, however, sediment bedload transport is of interest. Various bedload transport equations were developed in partially full pipes since part full flow is the common condition for storm sewer systems (Perrusquía and Nalluri, 1995; May, 1989; Acker 1996). However, when

considering the last submerged pipe scenario, the reliability of bedload transport equations based on part full condition should be tested. And the request for developing bedload transport in full pipe flow condition is presented when considering the last storm sewer pipe.

For the sediment deposition, the process of deposit built up was summarized by Butler et al. (2003). In recent years, the deposition development rate is gaining more and more attention. Lange and Wichern (2013) produced the sedimentation dynamics in combined sewer systems. However, the deposition build-up rate is not developed by previous literature. In this study, the sediment deposition rate can be approximately calculated through the experiment data.

4.2 Experimental procedure

The experimental arrangement, shown in Fig. 9, consists of a vertical water inlet, a bottom sump under the water inlet, a sand feeding inlet, a 6 m long Plexiglas pipe, and a water pond at the downstream end. Water was supplied by a pump and the flow rate was measured using a magnetic flow meter with a range from 6.5 to 22.5 L/s. The inlet pipe has a vertical drop with 150 mm diameter, which may create high flow velocity. Thus, a 350 mm deep sump under the vertical pipe provided some energy dissipation and suitable entrance condition for flow into the pipe. The sand inlet of diameter of 50 mm and height of 1480 mm, provided the sand for transport. The feeding rate was controlled by the total sand weight and the time of feeding. Next part is the Plexiglas pipe (6 m long and 184 mm in diameter). The slope of the Plexiglas pipe can be adjusted to study the sediment deposition behavior for slopes varying from 0.5 % to 2 %. The pipe slope was controlled by a mechanical jack located at the upstream end of the frame. The downstream pond was used to collect sand and the pond had a control device to provide ponding to submerge all the 6 m long pipe

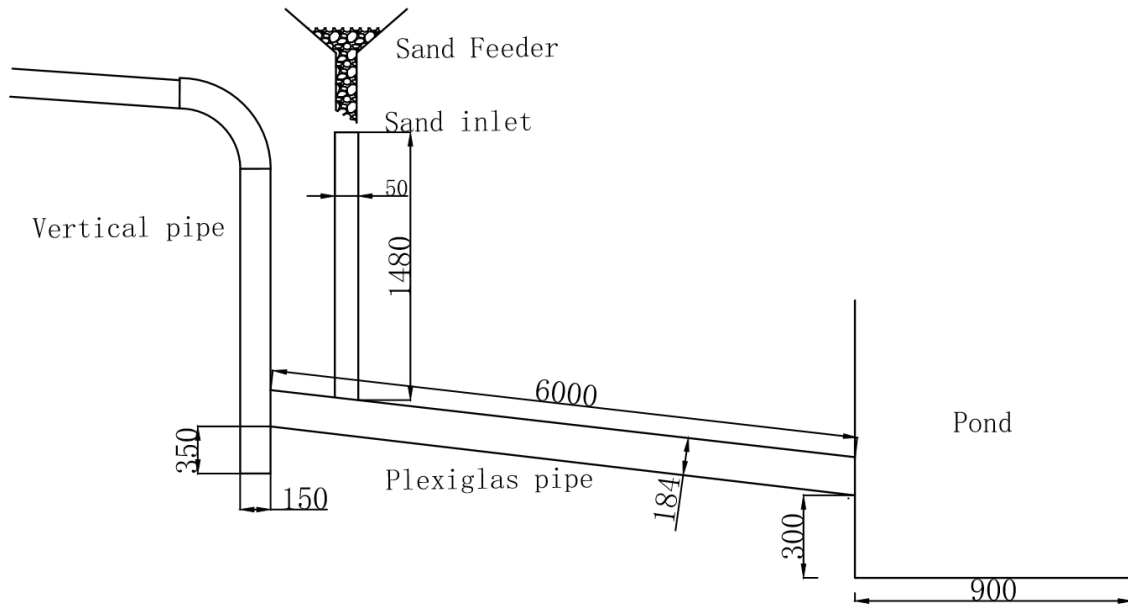


Figure 9. Experimental set up (unit: mm)

Two kinds of sediment were used in the tests (see Table 12 for detailed information): one is Sil 8/16 and the other is single particles of four sizes (5 mm, 10 mm, 20 mm, and 40 mm) by measuring the longest dimension of the particle. Single particles were used to test single particle travel velocity. All the test particles in single particle traveling velocity experiment were recycled to ensure the constant particle dimensions. Sil 8/16 was used to test deposition development. All particles had a 2.65 specific gravity.

Table 12. Particle information

Particle type	Size (mm)	Picture
Sil 8/16	Range: 0.04 - 2.40 <i>Cu</i> : 2.6 <i>d</i> ₅₀ : 1.80	
Single particle	5.00, 10.00, 20.00, and 40.00	

Two series of experiments were conducted subsequently, including single particle traveling velocity and sediment deposition development (detailed test parameters are shown in Table 13).

For the single particle traveling velocity experiment, the first step was to run water (6.5 L/s) in the set up (0.5% slope pipe) until downstream pond provided enough water level to submerge the pipe. For this steady state condition, the water flow rate was recorded. Different sizes of particles were added through the sand inlet and the traveling time (once particle contacts water and is finally flushed out into the pond) was recorded. The traveling velocity can be calculated from the traveling time and traveling distance (6 m). This procedure was repeated for different flow rates (10.5, 13, 17, and 19.5 L/s) and pipe slopes (1, and 2%).

For the sediment deposition development experiment, the preparation was the same as that of single particle velocity experiment. After the steady state condition set in (6.5 L/s in a 0.5% slope pipe), sand was added at a constant rate and the video camera started to record the deposition development. In this case, all added sand settled and thus this scenario can be used to calibrate the bulk density of sediment deposition in full pipe flow (bulk density equaled added sand weight by deposition volume). Since the sediment deposition volume in the submerged flow pipe was unable to directly measure, the sediment deposition cross sections along the center pipe line were plotted by AutoCAD (0.1 mm accuracy) based on the video recording. Assumed that the sediment deposition had flat surface and then extended the cross section to the pipe cylinder internal surface, the deposition volume can be obtained.

After the bulk density was obtained, tests for different flow rates (13 L/s and 19.5 L/s), pipe slopes (1% and 2%) and sand feeding rates were conducted. The test duration was 15 minutes for a sand adding rate of 5 g/s and the duration was 5 minutes for other cases when the deposition height stopped growing within the time duration.

Table 13. Experiment groups and tests
(a) Single particle traveling velocity experiment

Slope	0.5%, 1.0%, and 2.0%			
Water flow rate (L/s)	10.5	13	19.5	26
Flow velocity (m/s)	0.40	0.50	0.75	1.00
Sediment size (mm)	0.5	1	2	4

(b) Sediment deposition development experiment

Slope	0.5%, 1.0%, and 2.0%		
Water flow rate (L/s)	6.5	13	19.5
Flow velocity (m/s)	0.25	0.50	0.75
Sil 8/16 adding rate (g/s)	2.5	5, 15	22, 45

4.3 Single particle traveling velocity

Before discussing the single particle traveling velocity, an important scenario should be mentioned. When testing different sizes of particles in different flow rates and slopes, some particles settled instead of traveling. For 2% slope pipe, most test particles can move during all the flow velocity range except for the 40 mm particle with flow velocity less than 0.5 m/s. For 1% and 0.5% pipe, as long as flow velocity less than 0.75 m/s, all particles settled. Therefore, the pipe slope plays a significant role in particle traveling rates; that is, the single particle critical deposit velocity for 0.5% and 1% pipes is less than 0.5 m/s while for 2% pipe, it is less than 0.75 m/s.

The results of the particle velocity measurements under different pipe slopes and flow velocities are plotted in Figure 10. For the same particle size and pipe slope, data points from bottom to top represent particle velocities in flow velocities from 0.4, 0.5, 0.75 to 1.0 m/s. For certain particle size (e.g., 5 mm), 2% pipe can convey particles in a larger flow velocity range (4 recorded data

points corresponding to 0.4, 0.5, 0.75, and 1.0 m/s velocities). By contrast, 0.5% and 1% pipes only can convey particles for velocity over 0.75 m/s (only two data points). For 2.0% slope pipe, the particles have wide range of velocities when compared with other two slopes data sets.

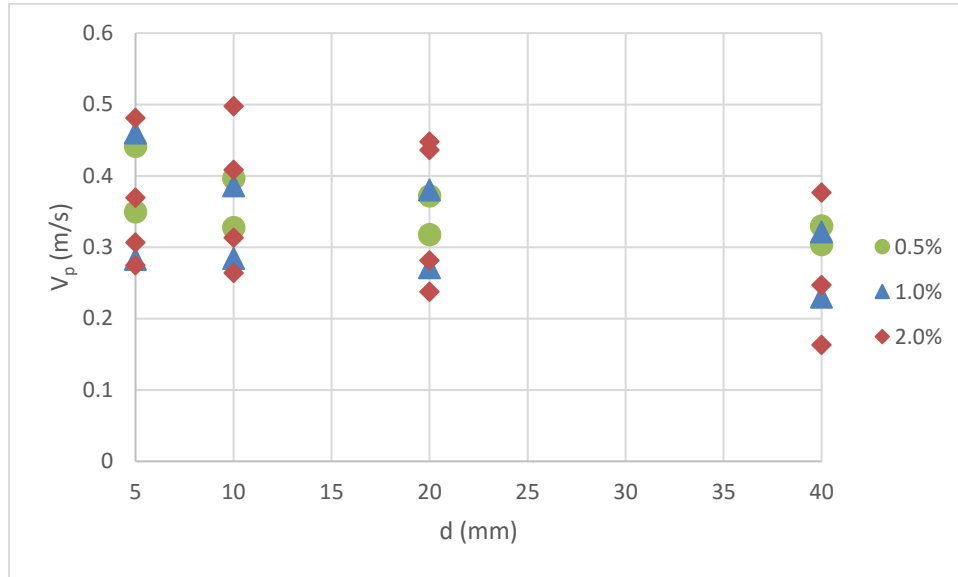


Figure 10. Particle velocity measurements

Ota and Perrusquía (2013) provided a method to use the relative particle velocity (ratio of particle velocity and mean flow velocity) and relative sediment size (ratio of particle size and pipe roughness) thereby developing prediction equation for particle traveling velocity which can be written as follows:

$$\frac{V_p}{V_m} = a_5(d_{50}/k)^{b_5} \quad (18)$$

where, V_p is the particle traveling velocity, V_m is the mean flow velocity, k is the pipe absolute roughness, and a_1 , b_1 are coefficients.

In this study, the pipe is Plexiglas which has a smooth surface. Thus, the pipe roughness is not significant compared to the particle size. Therefore, the pipe diameter was used to replace the pipe roughness:

$$\frac{V_p}{V_m} = a_6(d_{50}/D)^{b_6} \quad (19)$$

The original data were processed and a new dimensionless plot was obtained in Figure 11 (the ratio of particle velocity and mean flow velocity changes with the ratio of particle size and pipe diameter). As can be seen in Figure 11, the relative particle velocity decreases as the relative particle size increases in a pipe with certain slope. Also, the increase of pipe slope can increase the relative particle velocity (2% slope data set as a whole are higher than the groups of 1.0% and 0.5% slope data sets). Similar equation as Ota and Perrusquía's equation can be developed (see Table 14).

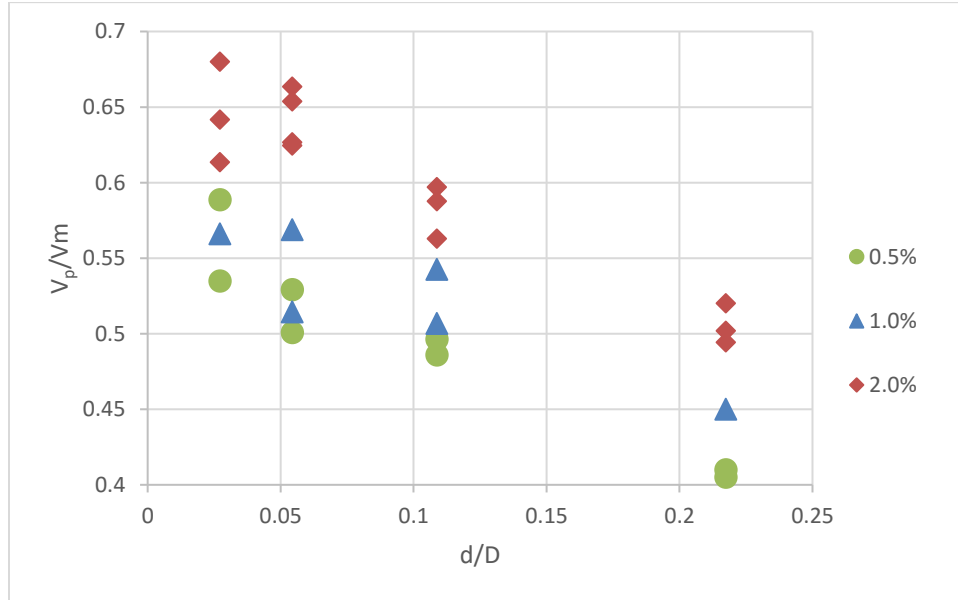


Figure 11. Single particle relative traveling velocity

Table 14. Single particle relative traveling velocity equations

Pipe slope	w_s/v_m equation	R^2	RMSE
0.5%	$\frac{V_p}{V_m} = 0.41(d_p/D)^{-0.093}$	0.65	2.4%
1.0%	$\frac{V_p}{V_m} = 0.46(d_p/D)^{-0.090}$	0.70	4.2%
2.0%	$\frac{V_p}{V_m} = 0.33(d_p/D)^{-0.162}$	0.92	1.7%

In general, the above equations have reasonable fit (over 0.65 R^2 and less than 5% RMSE). In detail, the 2% pipe has the best fitting of the particle velocity equation. The shallow pipe slope has a relatively stable velocity ratio at the same particle size (i.e., smaller dimensionless velocity difference between experimental data). While in steep pipe (2%), the velocity ratio has a large variation for the same particle size. This represents that steep pipe may convey particles in a wide range of flow velocities. The relative particle velocity in sediment transport over smooth pipe is as low as about 40% of the mean flow velocity.

After Table 14 has been developed, in order to incorporate the slope into the prediction equation, a multiple correlation has been applied. A new equation has been developed:

$$\frac{V_p}{V_m} = 0.72(d_p/D)^{-0.10} S^{0.12} \quad (20)$$

This equation has a RMSE of 3.5% and a 0.87 R^2 , which shows a good correlation. The relative particle velocity increases with relative particle size decreases and pipe slope increases.

4.4 Sediment deposition development

- Bulk density

In the case of 6.5 L/s flow rate and 2.5 g/s sand feeding rate, all added sand settled. Since the sediment deposition volume in the submerged pipe was unable to directly measure, the sediment deposition cross sections along the center pipe line were plotted by AutoCAD (0.1 mm accuracy)

based on the video recording. Assuming that the sediment deposition had flat surface and then extended across the cross section to the pipe cylinder internal surface, the deposition volume can be obtained. The blue volume in Figure 12 was the plotted sediment deposition volume. Using this method, all sediment deposition volumes can be measured in AutoCAD software.

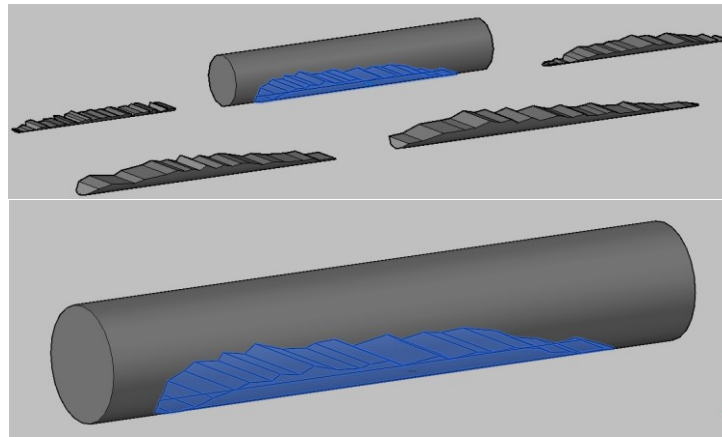


Figure 12. Sediment deposition volume plotted by AutoCAD

Since all the sand added to the system was deposited in the 6.5 L/s flow rate scenario, the bulk density equals the ratio of total added weight and plotted deposition volume (Figure 12). Table 15 summarizes all bulk densities. The mean bulk density is 1420 g/L with a standard deviation of 10, which shows the reliability of the calculations.

Table 15. Sediment bulk densities for 6.5 L/s flow rate scenario

Slope	0.5%	1.0%	2.0%	0.5%	1.0%	2.0%
Item	Volume (L)			ρ_b (g/L)		
1 min	0.10	0.12	0.12	1480	1300	1300
2 min	0.23	0.22	0.24	1300	1370	1260
3 min	0.28	0.31	0.29	1580	1450	1540
4 min	0.39	0.41	0.42	1520	1450	1440
5 min	0.52	0.51	0.53	1430	1460	1420
Mean				1420 \pm 10		

Based on the bulk density calculation, the sediment void ratio can be obtained. The bulk density equation is shown below:

$$\rho_b = \sigma\rho_w + (1 - \sigma)\rho_s \quad (21)$$

where σ is the sediment void ratio.

After calculation, σ equals 0.74 which is larger than the typical void ratio value (0.40 in descent water). This is likely due to the sediment volume over estimation. According to the observation, the realistic blue volume top surface (Figure 12) is more like a U shape instead of the assumed flat surface. Thus, the sediment deposition weight as well as the deposition development rate were overestimated, however, they can present the development tendency and general rules.

- Sediment deposition development pattern

Deposition development was studied after pipe deposition bulk density was obtained. Figure 13 illustrates the deposition height development as a time series. As can be seen in Figure 13, the development of deposition appears to have two stages: one in which the sand is deposited in both

height and length directions (called rapid develop stage) whereas in the other, deposition only grew in length direction and stopped growing in height (named equilibrium develop stage). Under the same flow velocity, the equilibrium point was reached faster as sand feeding rate increased (after 8 minutes the equilibrium stage formed for 5 g/s feeding rate scenarios, while 3 minutes are enough to form equilibrium for 15 g/s feeding rate scenarios). Also under the same flow velocity and pipe slope, the equilibrium height (dash lines) was the same despite different sand feeding rates. The equilibrium height decreases as the flow velocity increases and pipe slope increases.

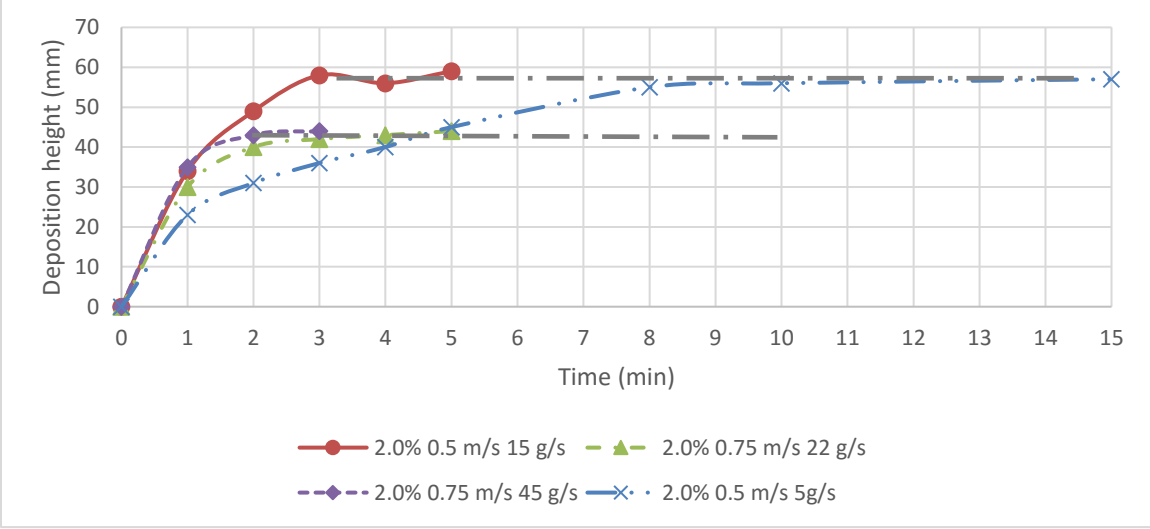
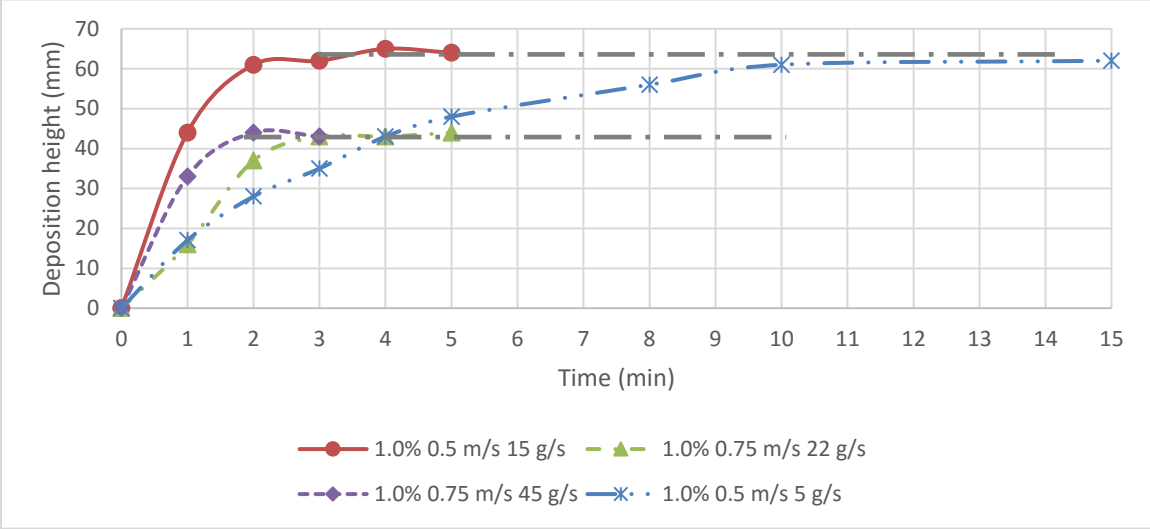
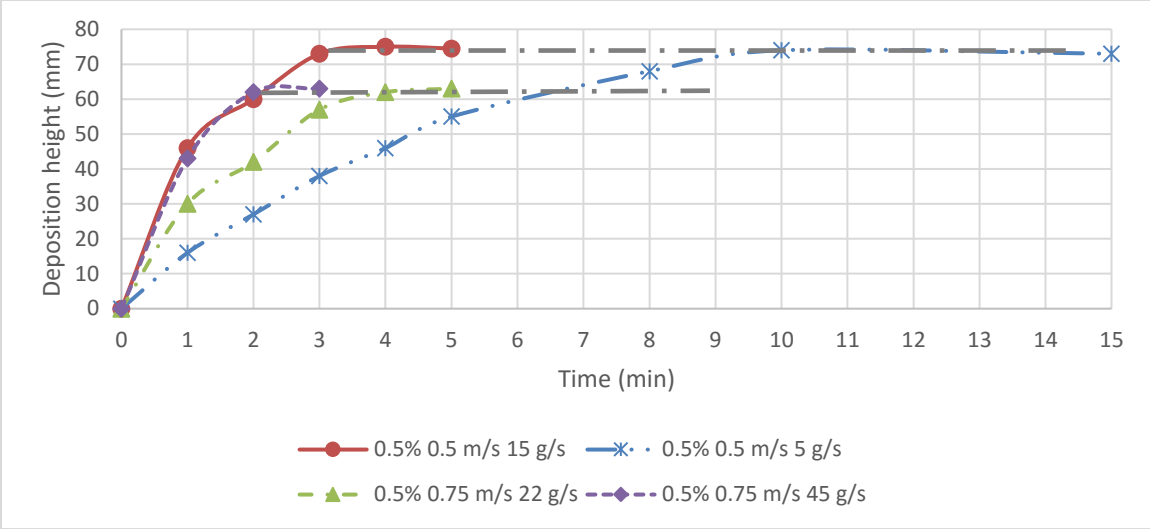


Figure 13. Sediment deposition development in height

Figure 14 and 15 illustrate the previous two development stages in both height and length directions. In Figure 14, only rapid development stages were shown. During this stage, the cross section shapes of every minute are roughly similar. The end point of all sand mounds are relatively stationary (within 5 cm), while the tip of the sand mound moved downstream with time. As the slope decreases, the sand mounds become more concentrated (with smaller length and higher height), while the flattest sand mound formed in the 2.0% slope pipe. The sand mound grew in both length and height directions.

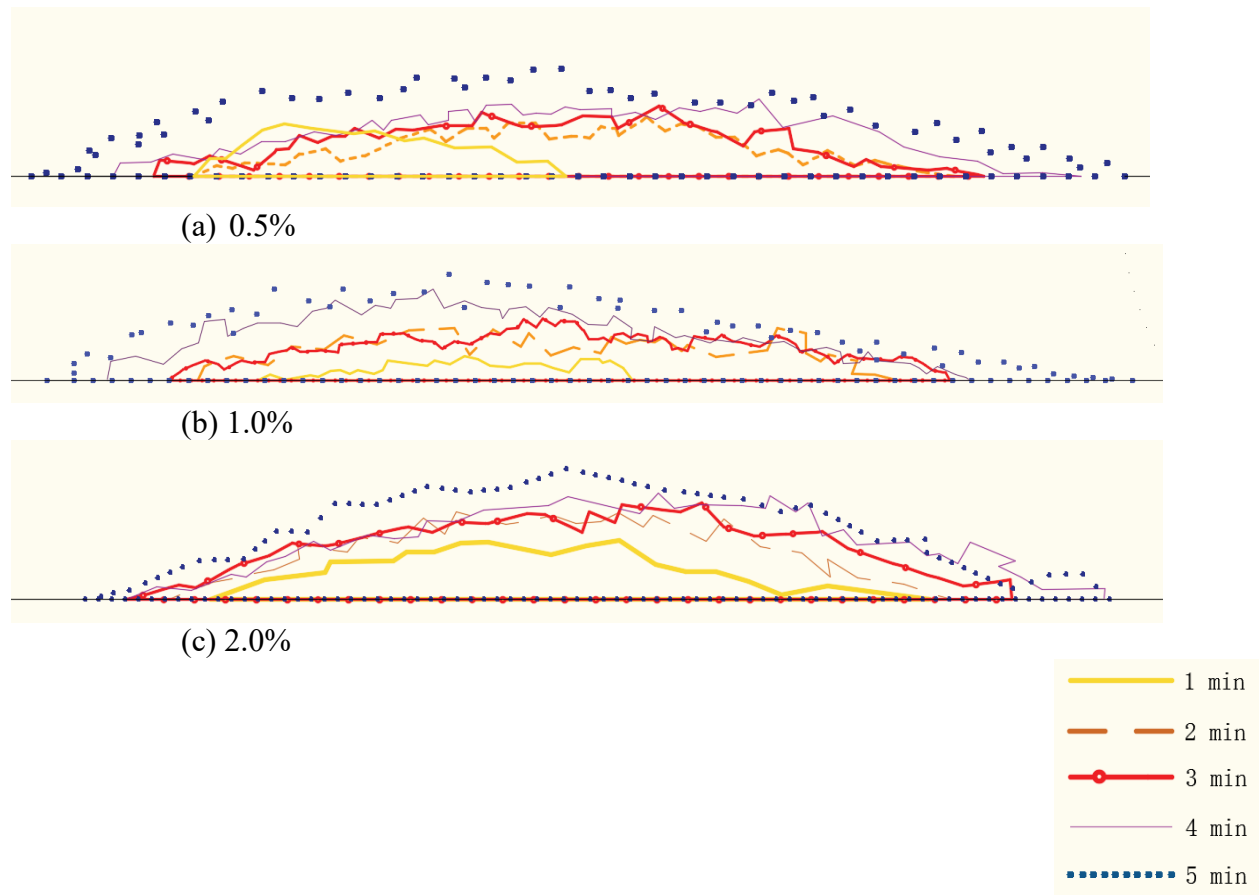


Figure 14. Sediment deposition rapid development stage (flow velocity 0.25 m/s and feeding rate 2.5 g/s)

The deposition development in Figure 15 contained both the rapid development stage and the equilibrium development stage. The first two minutes are the rapid development stage, during which, the sand mound cross sections were similar between 1 and 2 minute. When reached equilibrium development stage, the sand mound cross sections stopped growing in height direction. The sand mound tips moved relatively large distances (over 15 cm) during one minute. The sand mound end point sometimes moved forward and sometimes backward, which was quite unsteady.

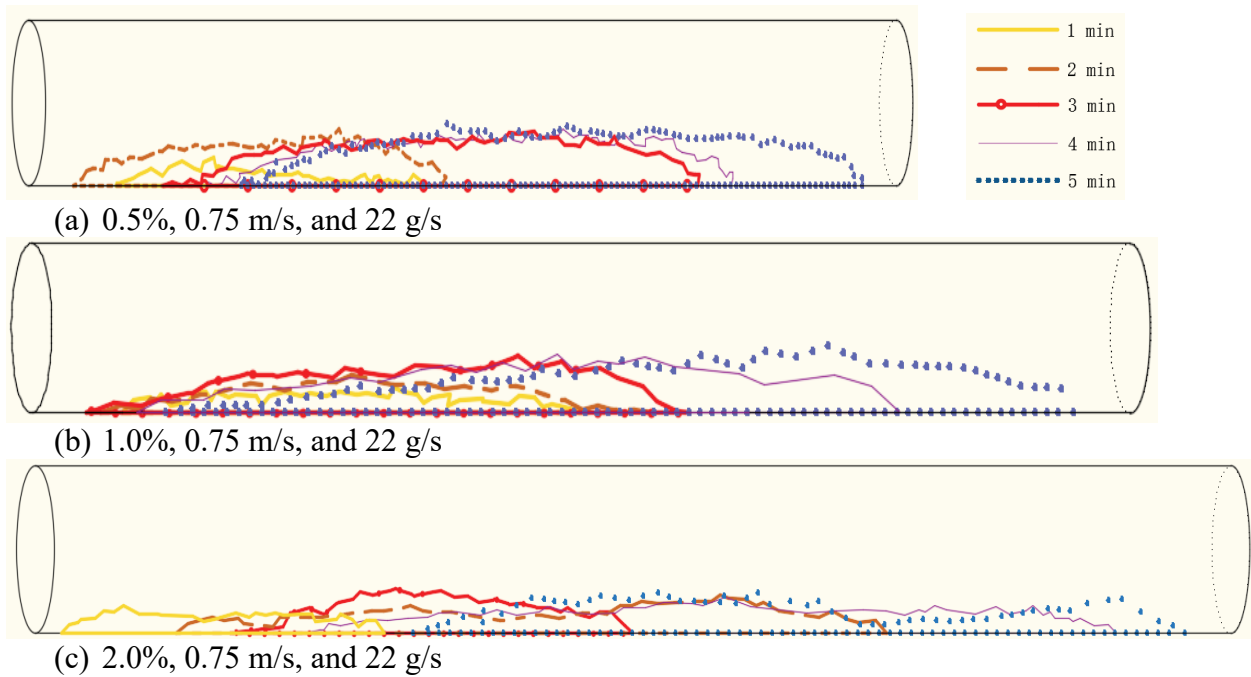
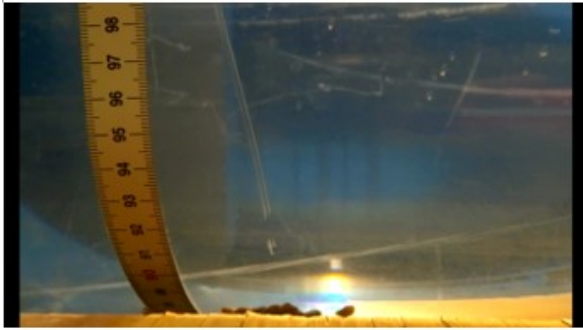
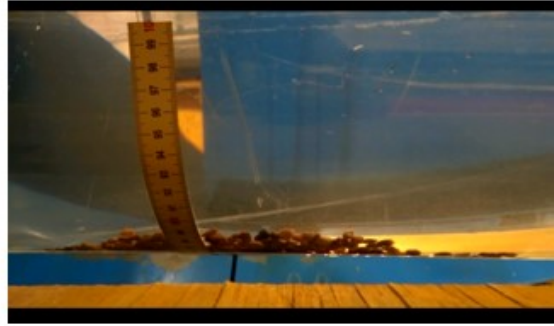


Figure 15. Sediment deposition development (including both rapid and equilibrium develop stages)

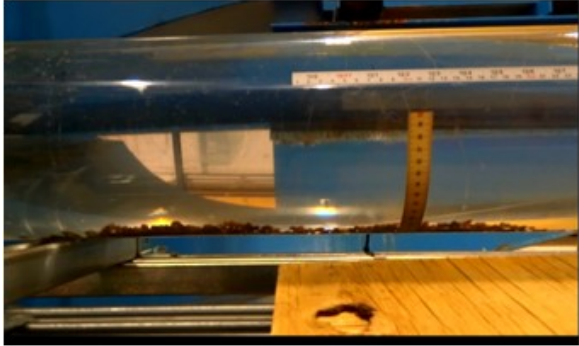
The following figures show the sediment deposition developments in different scenarios.



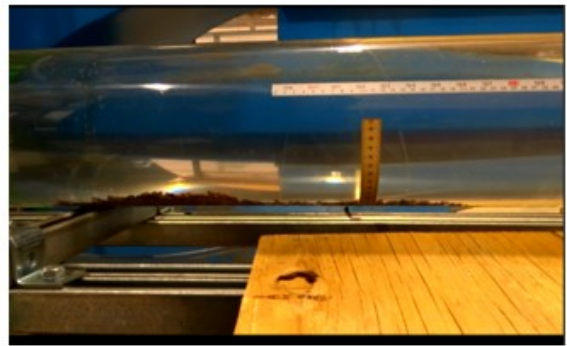
1min



2 min



3 min



4 min



5 min

Figure 16. Sediment deposition in 0.5% pipe with 0.5 m/s flow velocity and 5 g/s sand feeding rate



1 min



2 min



3 min



4 min



5 min

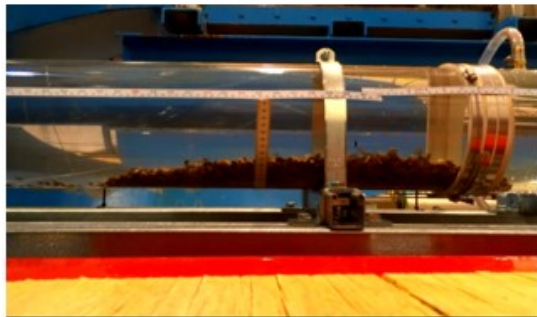
Figure 17. Sediment deposition in 0.5% pipe with 0.5 m/s flow velocity and 15 g/s sand feeding rate



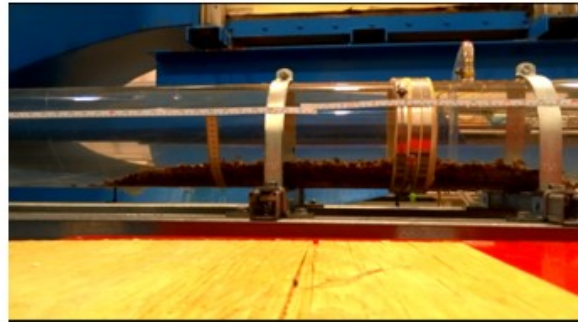
1 min



2 min



3 min

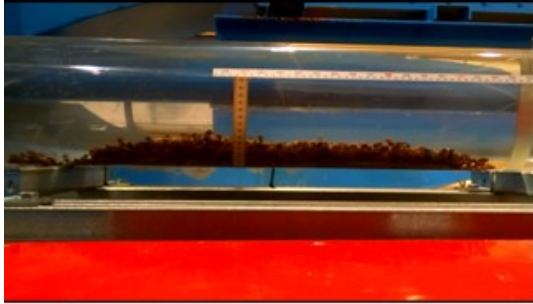


4 min



5 min

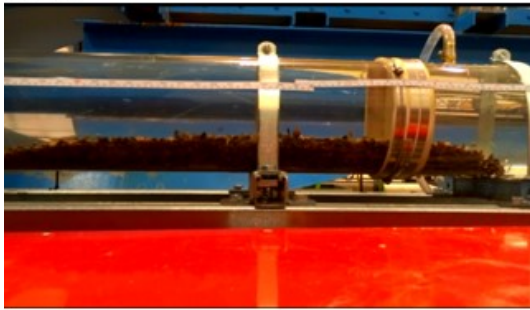
Figure 18. Sediment deposition in 0.5% pipe with 0.75 m/s flow velocity and 22 g/s sand feeding rate



1 min

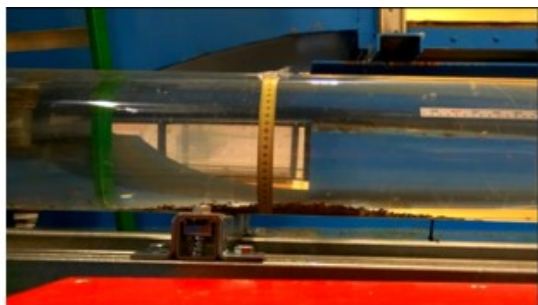


2 min

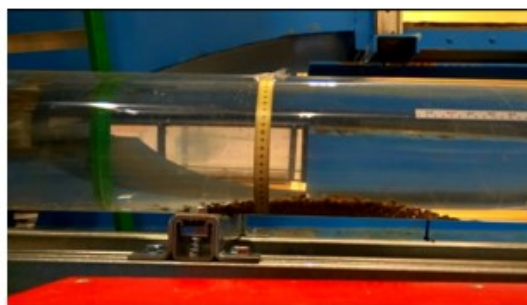


3 min

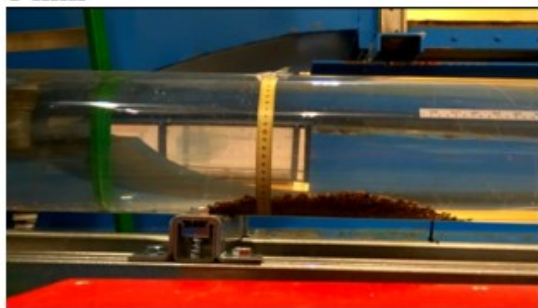
Figure 19. Sediment deposition in 0.5% pipe with 0.75 m/s flow velocity and 45 g/s sand feeding rate



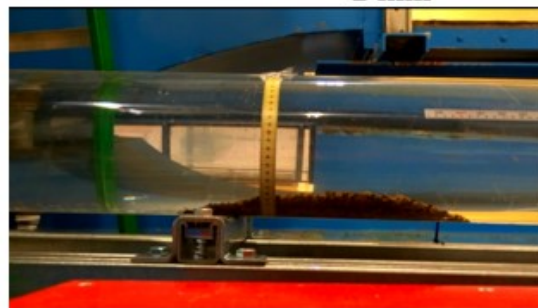
1 min



2 min



3 min

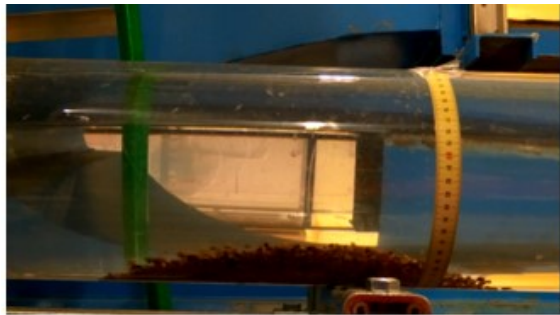


4 min

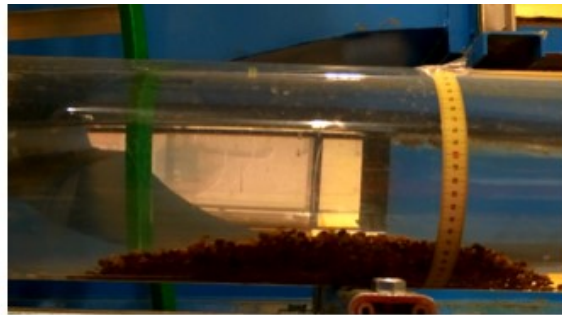


5 min

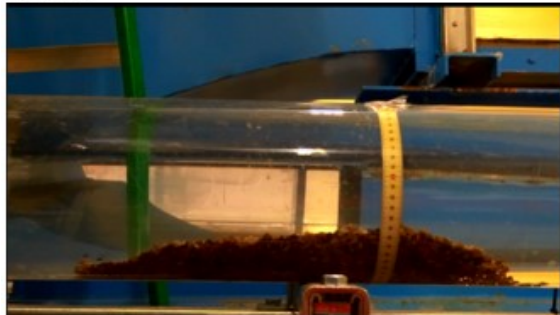
Figure 20. Sediment deposition in 1.0% pipe with 0.5 m/s flow velocity and 5 g/s sand feeding rate



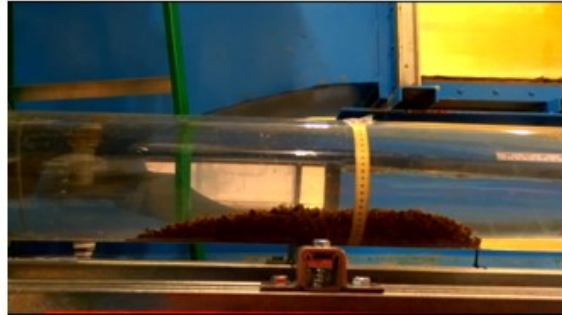
1 min



2 min



3 min



4 min

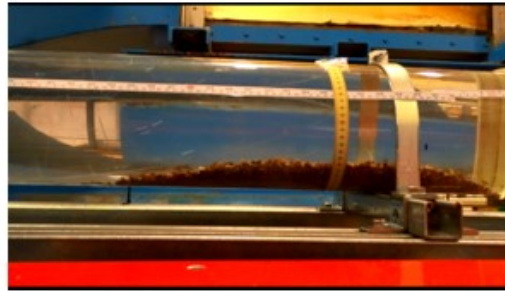


5 min

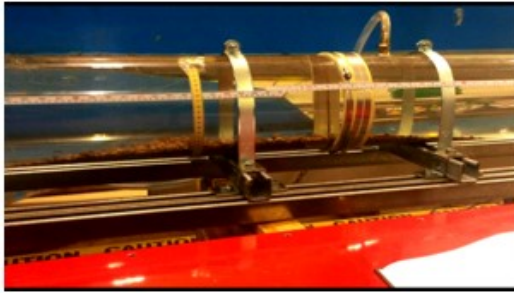
Figure 21. Sediment deposition in 1.0% pipe with 0.5 m/s flow velocity and 15 g/s sand feeding rate



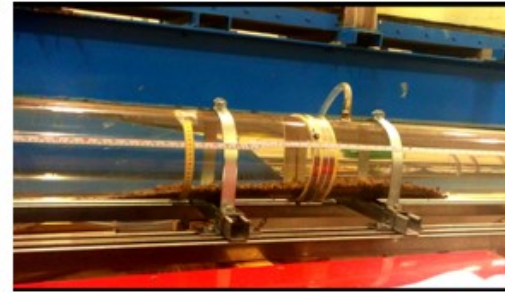
1 min



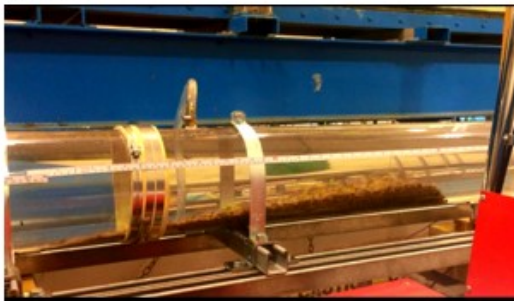
2 min



3 min

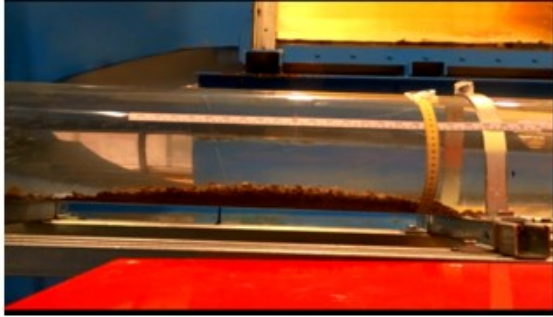


4 min

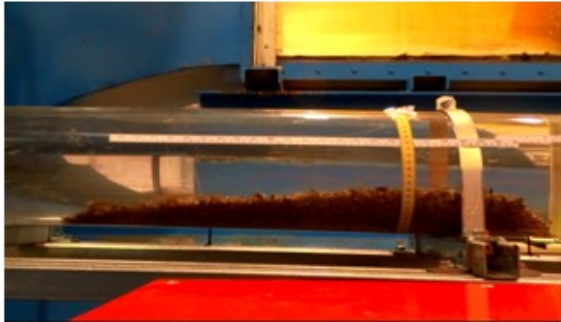


5 min

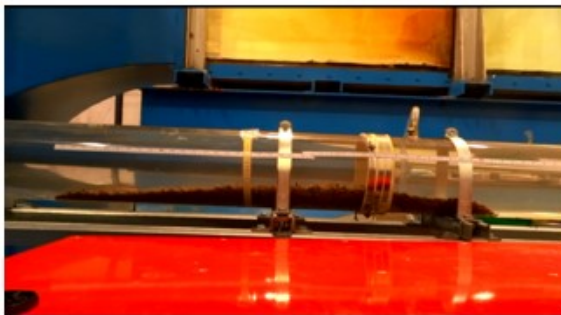
Figure 22. Sediment deposition in 1.0% pipe with 0.75 m/s flow velocity and 22 g/s sand feeding rate



1 min



2 min



3 min

Figure 23. Sediment deposition in 1.0% pipe with 0.75 m/s flow velocity and 45 g/s sand feeding rate



1 min



2 min



3 min



4 min



5 min

Figure 24. Sediment deposition in 2.0% pipe with 0.5 m/s flow velocity and 5 g/s sand feeding rate



1 min



2 min



3 min

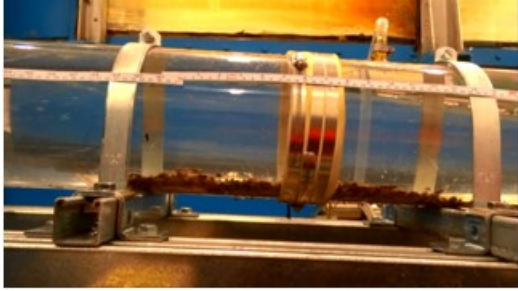


4 min



5 min

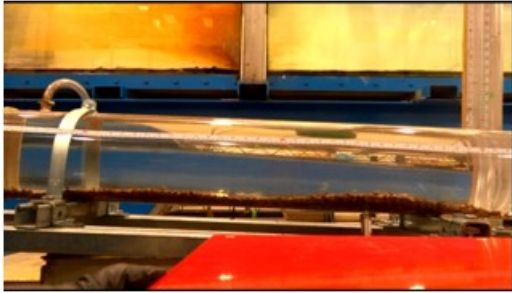
Figure 25. Sediment deposition in 2.0% pipe with 0.5 m/s flow velocity and 15 g/s sand feeding rate



1 min



2 min



3 min

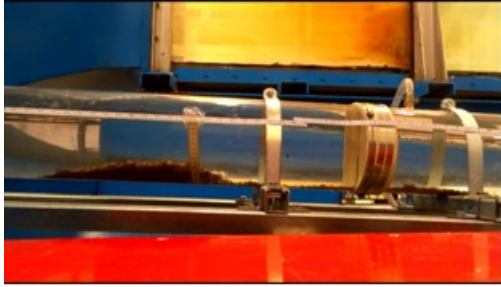


4 min

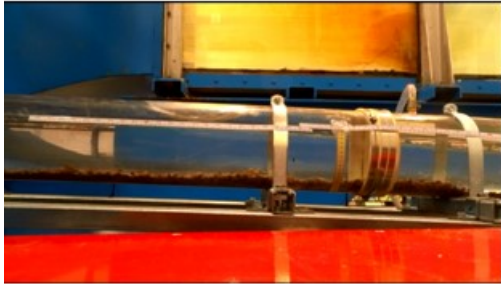


5 min

Figure 26. Sediment deposition in 2.0% pipe with 0.75 m/s flow velocity and 22 g/s sand feeding rate



1 min



2 min



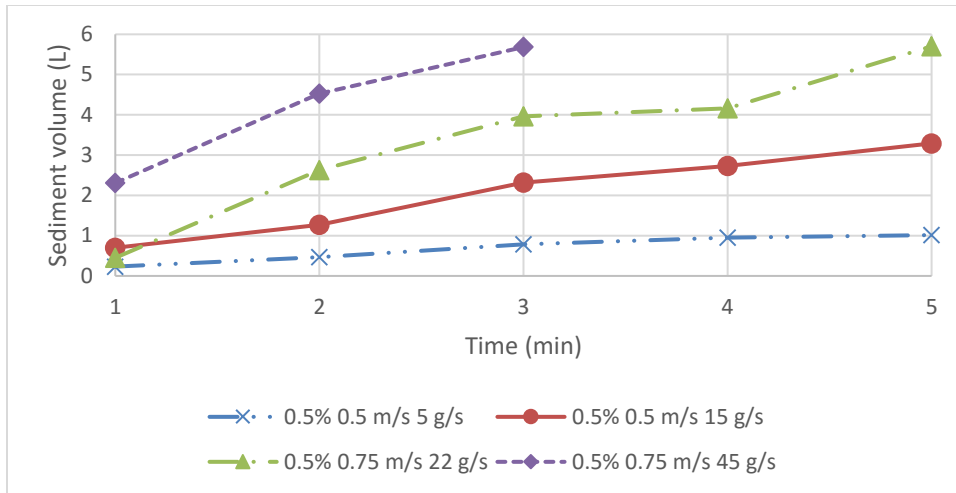
3 min

Figure 27. Sediment deposition in 2.0% pipe with 0.75 m/s flow velocity and 45 g/s sand feeding rate

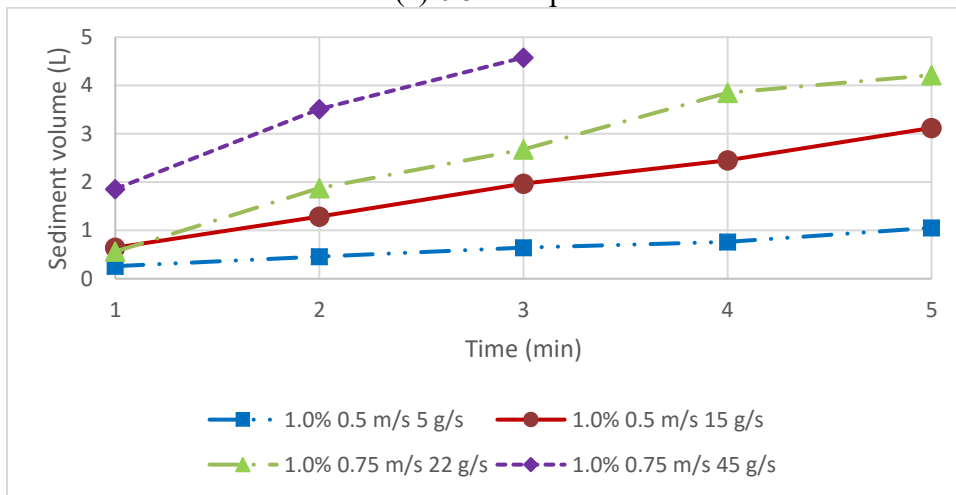
- Deposition development rate

The sediment deposition volumes are plotted in Figure 28. According to Figure 28, in general, the sediment deposition volume decreases as the pipe slope increases. This is mainly caused by the bed shear stress. Large slopes can produce large bed shear stresses which can convey more sediment and reduce the sediment deposition volume. Although different slopes can lead to different deposition volumes, the sediment deposition development patterns are similar among different slopes. For 5 g/s and 15 g/s feeding rate, all slope cases have nearly linear development with time (stable development rate). These are similar to stationary deposition development. The

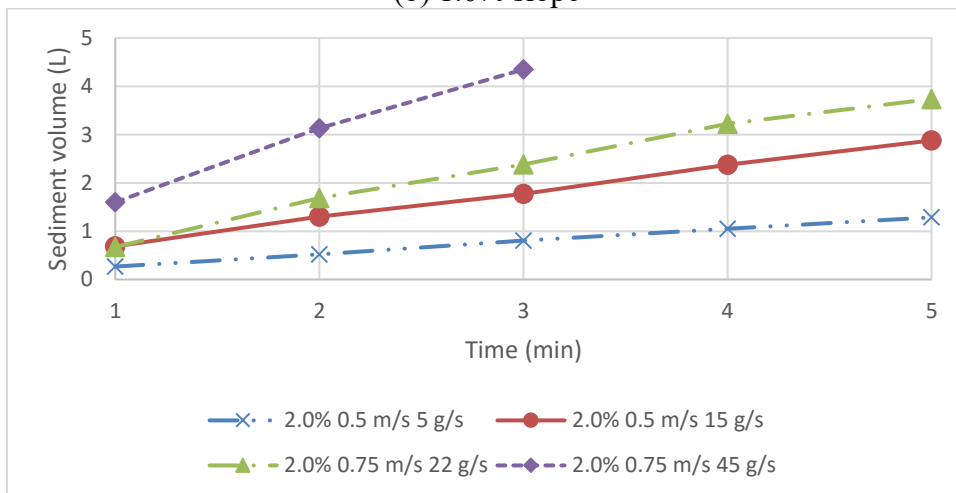
main reason is that the low flow velocity (0.5 m/s) only conveys a very small amount of sediment and therefore most sediment deposits. For 22 g/s feeding rate and with 0.75 m/s velocity, the development pattern is complicated, with a fluctuating development rate. For 45 g/s feeding rate and 0.75 m/s flow velocity, the first 2-minute period shows a significant sediment deposition development rate which is reflected by the steep slope. However, the following minute (2 – 3 min) has a reduced development rate, which corresponds to a large transport rate. This is mainly caused by the relatively large bed shear stress due to the thick deposition layer.



(a) 0.5% slope



(b) 1.0% slope



(c) 2.0% slope

Figure 28. Sediment deposition development in measured volume

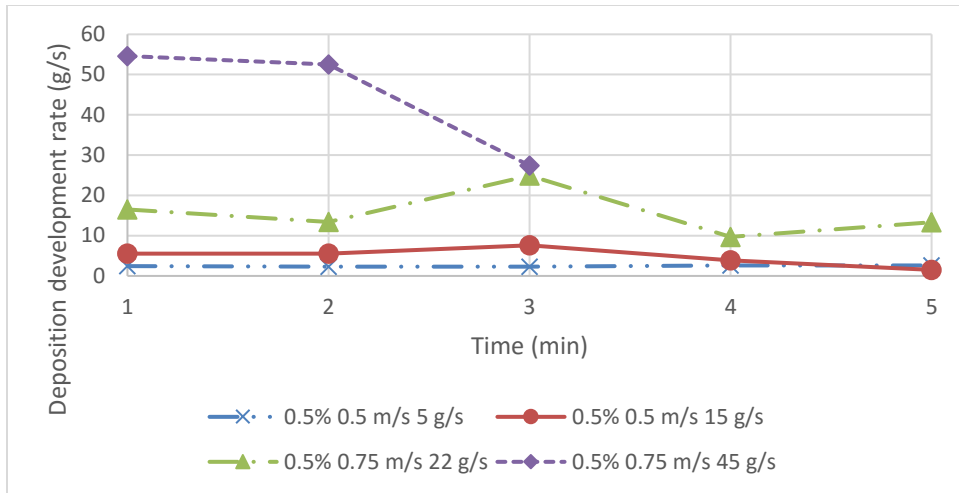
Then, the deposition development rate for every i^{th} minute can be calculated by:

$$W_i = \frac{(V_{d_{i+1}} - V_{d_i})\rho_b}{t_{i+1} - t_i} \quad (22)$$

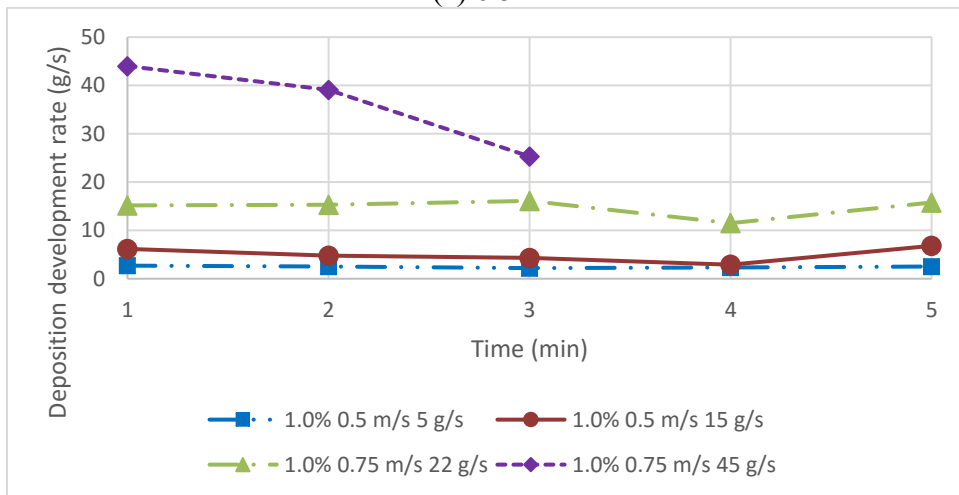
where, W is the deposition development rate, V_d is the deposition volume, ρ_b is the bulk density, t is time, and $i = 1, 2, 3, \dots$

All deposition development rates are plotted in Figure 29. As can be seen in Figure 29, most sand was deposited when sand adding rate was less than 45 g/s. Mean values of sediment deposition development rates are close to the sand feeding rate. Some values were even larger than the feeding rate, which is due to experiment errors and the assumption that all deposition layers were flat (in fact they were hollow). However, these deposition developments with 45 g/s sand feeding rate can represent the deposition development as well as sediment transport which is valuable to describe followed.

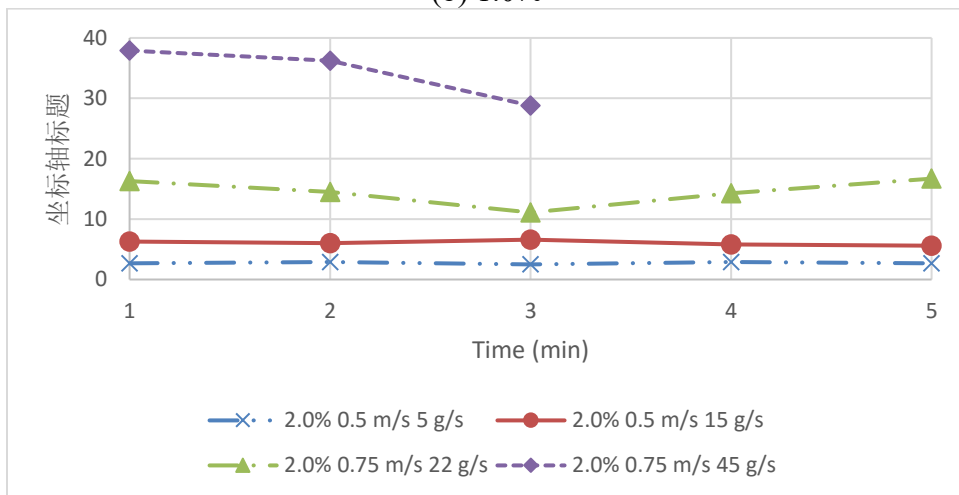
In 45 g/s scenario, the deposition development rates decrease as the pipe slope increases. It means that the steep slope can convey more sediment even at the same flow rate and reduce the sediment deposition development rate. In the same slope tests, the development rates also decreased with time. When compared this decrease to the deposition layer cross section plot, it is obvious that the higher the sand mound the smaller the sand development rate. This was mainly caused by the bed width and roughness increase. In general, the increasing deposition height and the pipe slope are the main reasons leading to the sediment transport capacity. In the following section, detailed discussion about sediment transport capacity is presented.



(a) 0.5%



(b) 1.0%



(c) 2.0%

Figure 29. Sediment development rate changes with time

4.5 Sediment transport capacity

According to the literature (Perrusquía, 1991; Ab Ghani, 1993), the dimensionless version of the transport function is given by “ π theorem” as:

$$\phi_b = f(\psi_b, d_*, s, Z, Y_r, t_r, k_r) \quad (23)$$

where, $\phi_b = \frac{C_s R_b V_m}{\sqrt{g(s-1)d_{50}^3}}$ (ϕ_b is transport parameter; C_s is the ratio of sediment transport volume

and flow rate; R_b is the hydraulic radius of the bed; g is gravitational acceleration; s is relative

density of the sediment; d_{50} is the sand median size). $\psi_b = \frac{(s-1)d_{50}}{R_b S}$ (ψ_b is bed shear intensity; S is

the pipe slope); $d_* = \left(\frac{g(s-1)}{v^2}\right)^{1/3} d_{50}$ (d_* is dimensionless particle number; v is kinematic

viscosity); $s = \rho_s / \rho$ (ρ_s is sediment density and ρ is water density); $Z = \frac{d_{50}}{Y}$ (Z is relative grain

size; Y is flow depth); $Y_r = Y/D$ (Y_r is relative flow depth; D is pipe diameter); $T_r = T/D$ (t_r is

relative bed thickness; T is sediment thickness); $k_r = d_{50}/k$ (k_r is relative pipe roughness).

Perrusquía focused on the sediment movement in part full pipe and concluded that bed mobility number, dimensionless particle number, relative flow depth and relative bed thickness were important factors to describe sediment transport capacity. In this study, pipe full flow is the main difference from the previous studies, therefore 5 of the above dimensionless parameters (d_*, s, Z, Y_r, k_r) are constant because of the full pipe flow and the same particle size distribution (flow depth Y , particle d_{50} ; particle density; water density; and pipe diameter are constant). Thus, the sediment transport capacity equation in this study can be determined by ϕ_b, ψ_b , and t_r . The general form of the equation is shown below:

$$\phi_b = c \psi_b^d t_r^e \quad (24)$$

where, c_1, d_1 , and e_1 are coefficients.

According to the sediment deposition development study, the sediment transport rate can be determined by the difference between the sand addition rate and the deposition development rate. As mentioned before, the deposition development rate is mainly determined by the slope and deposition shape, which also can be treated as factors that affect the sediment transport capacity. This is identical to the “ π theorem” (the sediment transport capacity equation in this study can be determined by ϕ_b , ψ_b , and t_r). Thus, the main concerns to calculate transport capacity are the sediment transport rate (volume), hydraulic radius of the sediment bed, and the sediment deposition thickness. The transport rate can be determined by the sand addition rate and the deposition development rate, thus, the sediment transport volume can be determined by: sediment transport rate/sediment bulk density. The general transport capacity is determined by the lowest transport capacity cross section. And the lowest transport capacity section has the widest bed width and highest bed thickness. These two parameters can also be measured in AutoCAD. In this study, deposition development rates (volume) for every minute might be obtained, therefore the transport capacity calculation is also based on minute duration.

In specific, C_s equals $\frac{(W_s - W_i)/\rho_b}{Q}$. In the previous term, W_s is the sand addition rate. The sediment thickness is measured by AutoCAD at the same cross section as the widest width section. The R_b , which is the most complicated factor, can be calculated based on AutoCAD plots. Subsequently, the relationship of transport capacity and dimensionless bed shear stress/relative bed thickness t_r were plotted in Figure 30 and 31.

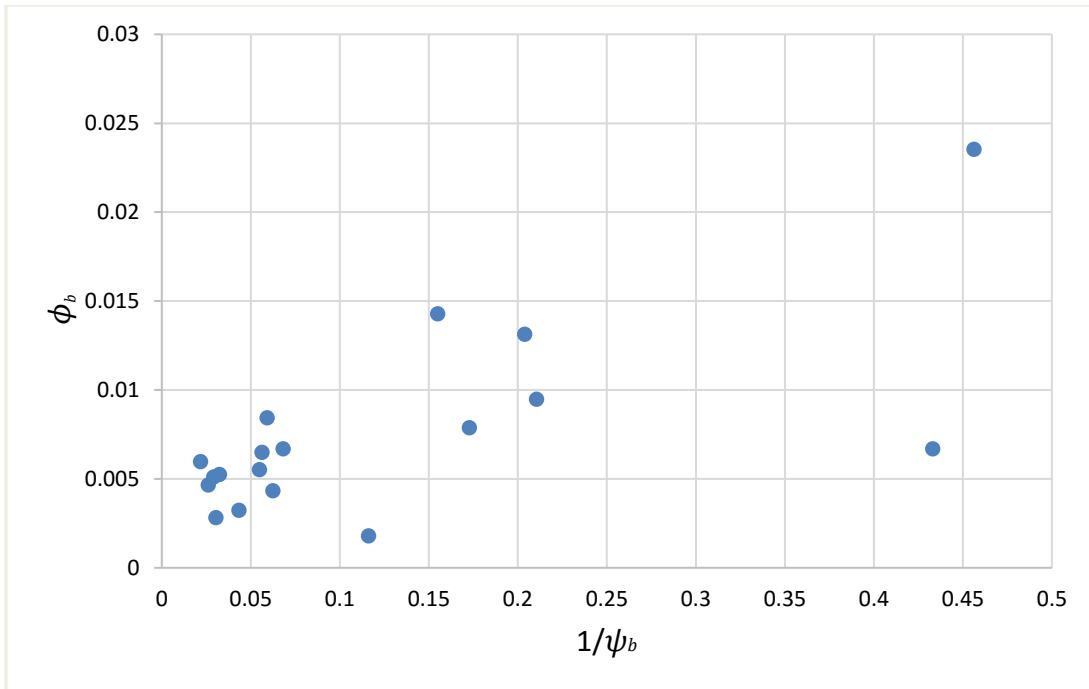


Figure 30. Sediment transport parameter changes with dimensionless bed shear stress

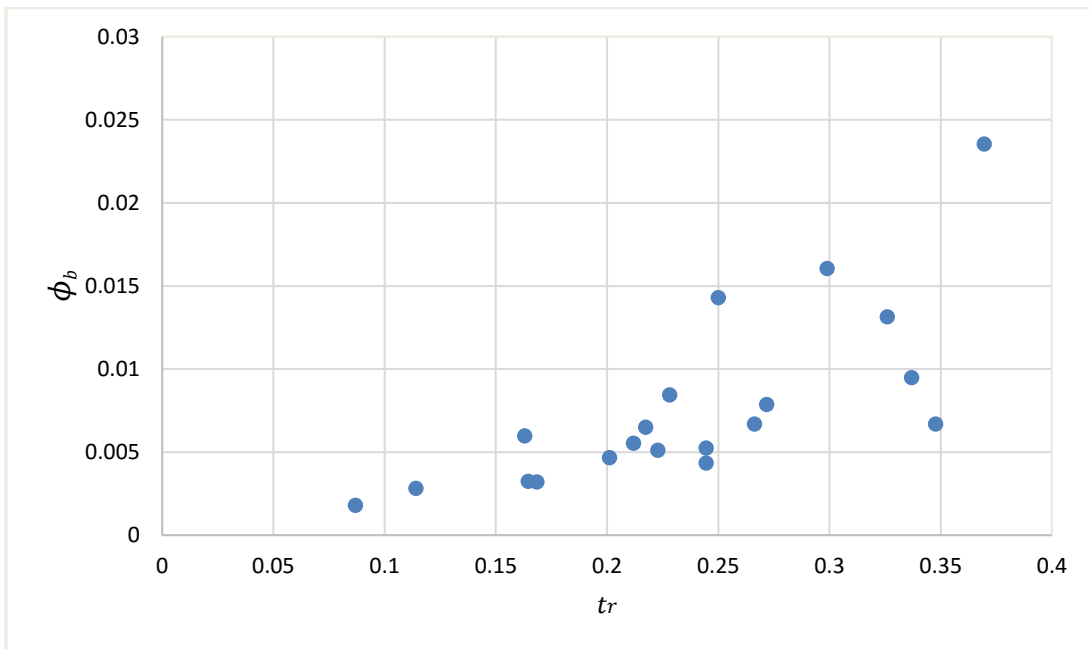


Figure 31. Sediment transport parameter changes with dimensionless bed thickness

As can be seen in Figure 30, the bed shear intensity seems to be sufficient to describe the sediment transport process. It is clear that shear stress plays an important role in the motion of particles and some of the sediment transport. In Figure 31, the correlation is clearer than Figure 30. In general, these two parameter are incorporated in the sediment transport function which is shown below: $\phi_b = 0.022\psi_b^{-0.23}t_r^{0.81}$. This equation has a RMSE of 0.1% and a correlation coefficient of 0.86, which represents a good description of the general characteristics of the sediment transport rate. When comparing the above equation to Table 6, the newly developed equation contains one more parameter (t_r) which can describe the influence caused by the bed deposition. In general, this equation has the same term as equations in Table 6, which presents the reliability of this equation to some extent.

4.6 Summary

In this study, the particle travel velocity and sediment deposition development are studied in submerged pipe. With respect to the particle travel velocity, the 2% pipe has the best fit to the particle velocity equation. The particle velocity in sediment transport over smooth pipe is as low as about 40% of the mean flow velocity, even for the fastest moving particle. Also, the particle velocity is a representation of the capacity of the flow to impose movement on sediment particles.

The development of deposition appears to have two stages, one in which the sand is deposited in both height and length directions (called the rapid development stage) and a second in which, the deposition only grows in the length direction and stops growing in height (named the equilibrium development stage). Under the same flow velocity, the equilibrium development stage forms faster as the sand feeding rate increases (after 8 minutes, the equilibrium stage formed for 5 g/s feeding rate scenarios, while 3 minutes were enough to form equilibrium for 15 g/s feeding rate scenarios).

Also under the same flow velocity and pipe slope, the equilibrium height (dash lines) is the same despite different sand feeding rates. The equilibrium height decreases as the flow velocity increases and pipe slope increases.

As for the sediment development rate, most of the sand was deposited when the sand addition rate was less than 45 g/s. Mean values for the sediment deposition development rate are close to the sand feeding rate. However, these deposition developments with a 45 g/s sand feeding rate can represent the deposition development as well as sediment transport. In the 45 g/s scenario, the deposition development rates decrease as slope increases at different pipe slope. Therefore, the steep slope can convey more sediment even at the same flow rate and reduce the sediment deposition development rate.

Finally, the sediment transport capacity can be described by an equation consisting of the sediment transport parameter, the dimensionless bed shear stress, and the relative bed thickness. The dimensionless bed shear stress seems to be sufficient to describe the sediment transport process. The relative bed thickness presents a good correlation to describe the sediment transport process as well. The proportional relationship between transport capacity and dimensionless bed shear stress/ relative bed thickness represents that with pipe slope increase and particle size decrease the sediment transport capacity can increase.

Chapter 5: Conclusions and Recommendations

In this thesis, a literature review on sediment in storm sewers was presented. Then, two sets of experiments were conducted in the T. Blench Hydraulic laboratory at the University of Alberta. The first experiment focused on the sediment capture efficiency in catchbasins, and the second experiment focused on the sediment movement in submerged pipes. Some conclusions and recommendations are listed below.

5.1 Conclusions

- *Storm sewer sediment characteristics and movement*

In chapter 2, storm sewer sediment comes from a number of possible sources: atmospheric deposition, wash-off from the surfaces within the catchment, sewer pipes themselves and construction sites. A storm sewer sediment classification method was developed by Roesner and Kidner mainly based on particle sizes. Particle size distributions in stormwater runoff have received significant attention; however, particle size information in sediment deposits in storm sewer pipes or catchbasins is still very limited. Particle median size and mode size can be used to describe the size feature of a group of sediment. Though particle median size is more widely used, the mode size can be more stable and representative. Sediment loading can be calculated if enough data including initial sediment on urban surface, the rain intensity, and the rainfall duration are available. Sediment movement includes three parts: erosion, transport and deposition. In terms of sediment blockage problems, sediment critical erosion velocity and sediment self-cleansing velocity are important parameters. Also, a collection of different experiments about sediment movement in storm sewers is presented in this thesis.

- *Catchbasin hydraulic features*

In chapter 3, compared to a catchbasin without a sump, a sump neither changes the water depth in the catchbasin relative to the invert of the outlet pipe nor changes the water depth in the outlet pipe. However, the presence of ICDs increases the water depth significantly. Orifice-type equations represent the “With ICD” scenario appropriately and can therefore be used for design purposes. As to energy dissipation, the amount of dissipation decreases with increasing discharge rate. However, given that it is over 60% in all cases, the energy dissipation is relatively high.

- Sediment capture efficiency

In terms of sediment capture efficiency, it decreases as the discharge rate increases as to be expected, and is greatest for coarser sediments. The presence of a sump improves the sediment capture efficiency, especially for larger particles. The presence of ICDs has a minor influence on the sediment capture efficiency for the smaller particles (62 μm d_{50} glass beads, 100 μm and 200 μm d_{50} sands) at small discharge rates.

- Sediment capture efficiency prediction

A new general expression was developed for predicting sediment capture efficiencies. This expression was used to generate four separate functions reflecting the three scenarios examined as well as the earlier studies, all of which have relatively high correlation coefficients and small *RMSE*. The new expression can be applied for a wide range of flow rates, water levels and particle sizes. In general, the new expression is clear and simple since it only requires direct physical parameters including W , Q , l , D_{out} and w_s , thus making it quite convenient to apply in urban drainage design.

- Particle traveling velocity

In chapter 4, the 2% pipe has the best fitting of the particle velocity equation. The 0.5% pipe slope has relatively stable velocity ratio for the same particle size group. The particle velocity in sediment transport over smooth pipe is as low as about 40% of the mean flow velocity, even for the fastest moving particle.

- Sediment deposition development

There are two patterns for sediment development (including stationary development and mobile development). As for sediment development rate, most sand was deposited when the sand addition rate was less than 45 g/s. Sediment deposition development rate mean values are close to the sand feeding rate. Deposition developments with 45 g/s sand feeding rate can represent the deposition development as well as sediment transport.

- Sediment transport capacity

Sediment transport capacity can be described by an equation consisting of the sediment transport parameter, the dimensionless bed shear stress, and the relative bed thickness:

$$\phi_b = 0.022\psi_b^{-0.23}t_r^{0.81}.$$

According to experimental data plots, the dimensionless bed shear stress seems to be sufficient to describe the sediment transport process. The relative bed thickness presents a good correlation to describe the sediment transport process as well. The proportional relationship between transport capacity and dimensionless bed shear stress or relative bed thickness shows that with pipe slope increase and particle size decrease the sediment transport capacity can increase.

5.2 Recommendations

- Reliable predictions for sediment loading and sediment characteristics

In order to obtain reliable predictions of the sediment loading entering storm sewer systems, further studies are need to relate these to catchment characteristics and stormwater events. In detail, the rainfall intensity data, catchment types, catchment surface sediment amount, catchment slopes, and the winter sanding amount should be collected. In field sampling, sediment physical and chemical characteristics need to be collected and analyzed at various key locations. The correlations and prediction models shall then be developed for practical use.

- Improving sediment capture efficiency at catchbasins

Firstly, laboratory modeling and field monitoring should be conducted to better understand the current performance of various designs of catchbasins. Then some possible design improvements should be tested in both experimental and practical catchbasins. Large flow rates close to the field flows should be applied in these studies. Studies to identify key locations for the placement of grit separators will also be of interest. In addition, through lab work, efficient cleaning methods can be developed for reducing the time/resources of cleaning thousands of catchbasins.

- Critical erosion velocity and self-cleansing velocity

In order to obtain representative d_{50} or mode size of sediment in sewers, field survey should be conducted on the size distributions of in-sewer sediment deposits. These values are indispensable to calculate critical erosion velocity and self-cleansing velocity. Hydraulic conditions including steep slopes, intermittent flows, and particle consolidation should be incorporated to develop predictive equations. Simultaneously, flow monitoring as well as deposition observation at various key locations are needed to test the reliability of applying critical erosion velocity or self-cleansing velocity to design storm sewers under real world conditions.

- Experimental and numerical study on sediment transport and deposition

The experimental part will study the sediment transport and deposition in storm sewers with a wide range of sediment concentrations, pipe sizes, pipe slopes, and pipe roughness, as well as the effect of bed deposition. A related numerical model will also be constructed for simulating sediment movement and development in storm sewers. These studies can provide information on: sediment mound dimension prediction and sediment movement over deposit bed; sediment deposition development rate which reflects the necessary sediment cleaning frequency; sediment transport capacity among existing pipe and flow conditions; and sediment deposit locations which may guide a City Operations team on sediment cleaning, sewer inspection, emergency repairs, etc.

- City operation and maintenance

For a better regulation of storm sewer systems, City Operation and Maintenance Team could follow the steps: firstly, conduct field investigation on sewer deposition size distributions and obtain the mode size; secondly, adjust catchbasin structures (i.e., sump depths or ICD sizes) to remove those sediments around mode size; thirdly, based on the deposition location prediction, clean related sewers for a certain frequency.

References

- Ab Ghani, A. (1993). Sediment transport in sewers. PhD thesis. University of Newcastle upon Tyne, England.
- Ackers, P. (1984). Sediment transport in sewers and the design implications. In Prof. of Int. Conf. On the Planning, Construction, Maintenance and Operation of Sewerage Systems, Cranfield BHRA The Fluid Engineering Centre.
- Ackers, J. C., Butler, D., and May, R. W. P. (1996). Design of sewers to control sediment problems. CIRIA Rep. No. R141, CIRIA, London.
- Alberta Environment. (1999). Alberta user guide for waste managers. Manifest Form 3/95, Part 2-5. Edmonton: Alberta Environment - Environmental Protection.
- Almedeij, J., Ahmad, E., & Alhumoud, J. (2010). Representative particle size of sediment in storm sewer inlets. *American Journal of Environmental Sciences*, 6(4), 316.
- American Society for Testing and Materials, ASTM (1992) Standard Classification. Soil Classification System (ASTM D 2487-92). ASTM, Philadelphia.
- Arbour, R. and Kerri, K. (1997). Collection Systems: Methods for Evaluating and Improving Performance. Prepared for the EPA Office of Wastewater Management by the California State University, Sacramento, CA.
- Aronson, G., Watson, D., & Pisano, W. (1983). Evaluation of catchbasin performance for urban stormwater pollution control. US EPA. Grant No. R-804578. EPA-600/2-83-043. Cincinnati.
- Aryal, R. K., & Lee, B. K. (2009). Characteristics of suspended solids and micropollutants in first-flush highway runoff. *Water, Air, & Soil Pollution: Focus*, 9(5-6), 339-346.

- Ashley, R. M., & Crabtree, R. W. (1992). Sediment origins, deposition and build-up in combined sewer systems. *Water Science and Technology*, 25(8), 1.
- Ashley, R. M., Arthur, S. S., Coghlan, B. P., & McGregor, I. I. (1994). Fluid sediment in combined sewers. *Water Science and Technology*, 29(1-2), 113-123.
- Ashley, R. M., & Hvitved-Jacobsen, T. (2002). Management of sewer sediments. R. Field, & D. Sullivan (Eds.). CRC Press/Lewis Publishers, Boca Raton, FL.
- Ashley, R., & Verbanck, M. (1996). Mechanics of sewer sediment erosion and transport. *Journal of Hydraulic Research*, 34(6), 753-769.
- Ashley, R., Bertrand-Krajewski, J., & Hvitved-Jacobsen, T. (2005). Sewer solids - 20 years of investigation. *Water Science and Technology*, 52(3), 73-84.
- ASTM International (2012). C1746/C1746M-12 Standard test method for measurement of suspended sediment removal efficiency of hydrodynamic stormwater separators and underground settling devices, West Conshohocken, PA, 2012, http://dx.doi.org/10.1520/C1746_C1746M-12.
- Azamathula, H. M. D., Ghani, A. Ab., and Yen Fei, S. (2011), ANFIS based approach for predicting sediment transport in clean sewer, *Applied Soft Computing* 12(2012) 1227-1230.
- Bai, S., & Li, J. (2012). Sediment wash-off from an impervious urban land surface. *Journal of Hydrologic Engineering*.
- Bertrand-Krajewski, J. L., Bardin, J. P., & Gibello, C. C. (2006). Long term monitoring of sewer sediment accumulation and flushing experiments in a man-entry sewer. *Water Science and Technology*, 54(6/7), 109-117.

- Bertrand-Kraiewsk, J., Scrivener, O., & Briat, P. (1993). Sewer sediment production and transport modelling – a literature review. *Journal of Hydraulic Research*, 31(4), 435-460.
- Bong, C., Lau, T., & Ghani, A. (2014). Sediment size and deposition characteristics in Malaysian urban concrete drains - a case study of Kuching City. *Urban Water Journal*, 11(1), 74-89.
- Boogaard, F. C., van de Ven, F., Langeveld, J. G., & van de Giesen, N. (2014). Stormwater Quality Characteristics in (Dutch) Urban Areas and Performance of Settlement Basins. *Challenges* (20781547), 5(1), 112-122.
- Brodie, I. M. (2006). Prediction of stormwater particle loads from impervious urban surfaces based on a rainfall detachment index. In *Proceedings of the 7th International Conference on Urban Drainage Modelling and the 4th International Conference on Water Sensitive Urban Design* (Vol. 1, pp. 27-34). Monash University.
- Butler, D. D., Davies, J. W., Jefferies, C. C., & Schütze, M. M. (2003). Gross solid transport in sewers. *Proceedings of ICE: Water & Maritime Engineering*, 156(2), 175-183.
- Butler, D., & Davis, J. W. (2011). *Urban drainage*. London; New York: Spoon Press.
- Butler, D., and Karunaratne, S. H. P. G. (1995). The suspended solids trap efficiency of the roadside gully pot. *Water Research.*, 29(2), 719–729.
- Butler, D., May, R., & Ackers, J. (2003). Self-cleansing sewer design based on sediment transport principles. *Journal of Hydraulic Engineering*, 129(4), 276-282.
- Characklis, G. W., & Wiesner, M. R. (1997). Particles, metals, and water quality in runoff from large urban watershed. *Journal of Environmental Engineering*, 123(8), 753-759.
- Chen, J., & Adams, B. J. (2006). A framework for urban storm water modeling and control analysis with analytical models. *Water resources research*, 42(6).

- City of Calgary. (2011). Stormwater management and design manual. Calgary, (http://www.calgary.ca/PDA/pd/Documents/urban_development/bulletins/2011-stormwater-management-and-Design.pdf).
- City of Calgary. (2013). Storm drainage system – FAQ. From <http://www.calgary.ca/UEP/Water/Pages/Water-and-wastewater-systems/Storm-drainage-system/Storm-Drainage-System-FAQ.aspx>.
- Clegg, S., Forster, C. F., & Crabtree, R. W. (1992). Sewer sediment characteristics and their variation with time. *Environmental technology*, 13(6), 561-569.
- Egodawatta, P., Thomas, E., & Goonetilleke, A. (2007). Mathematical interpretation of pollutant wash-off from urban road surfaces using simulated rainfall. *Water Research*, 41(13), 3025-3031.
- El-Zaemey, A. K. S. (1991) Sediment transport over deposited bed sewers, Ph.D. thesis, University of Newcastle upon Tyne.
- Fan, C. Y. (2004). Sewer sediment and control: a management practices reference guide. United States Environmental Protection Agency, Office of Research and Development, National Risk Management Research Laboratory, Water Supply and Water Resources Division, Urban Watershed Management Branch.
- Ferguson, R. I., & Church, M. (2004). A simple universal equation for grain settling velocity. *Journal of sedimentary Research*, 74(6), 933-937.
- Goncalves, C., Seters, T. V. (2012). Characterization of particle size distributions of runoff from high impervious urban catchments in the Greater Toronto Area. Toronto and Region Conservation.

- Graf, W. H., Acaroglu ER. (1968) Sediment transport in conveyance systems (Part 1): a physical model for sediment transport in conveyance systems. *Hydrol Sci J* 13(2):20–39.
- Graf, W. H. (1971) *Hydraulics of sediment transport*. McGraw-Hill, New York.
- Grottker, M. (1990). Pollutant removal by gully pots in different catchment areas. *Science of the total environment*, 93, 515-522.
- He, C. and Marsalek, J. (2014). Enhancing sedimentation and trapping sediment with a bottom grid structure. *J. Environ. Eng.*, 10.1061/(ASCE)EE.1943-7870.0000774.
- Howard, A. K., Mohseni, O., Gulliver, J. S. & Stefan, H. G. (2012). Hydraulic analysis of suspended sediment removal from storm water in a standard sump. *Journal of Hydraulic Engineering – ASCE* 138 (6), 491–502.
- Howard, A., Mohseni, O., Gulliver, J. & Stefan, H. (2011). SAFL baffle retrofit for suspended sediment removal in storm sewer sumps. *Water Research* 45 (18), 5895–5904.
- International Organization for Standardization (2002) *Geotechnical investigation and testing – identification and classification of soil*. ISO 14688-1.
- Kang, J. H., Kayhanian, M., & Stenstrom, M. K. (2006). Implications of a kinematic wave model for first flush treatment design. *Water research*, 40(20), 3820-3830.
- Lager, J. (1977). *Catchbasin technology overview and assessment*. US EPA. Contract No. 68-03-0274. EPA-600/2-77-051. California.
- Lange, R. L., & Wichern, M. M. (2013). Sedimentation dynamics in combined sewer systems. *Water Science and Technology*, 68(4), 756-762.
- Laplace, D., Bachoc, A., Sanchez, Y., & Dartus, D. (1992). Trunk sewer clogging development – description and solutions. *Water Science and Technology*, 25(8), 91-100.

- Letourneau, R., Amell, B., Deong, Y., and Wouts, R. (2008). City of Calgary stormwater quality retrofit program. Proceeding of 11th International Conference on Urban Drainage, Edinburgh, Scotland, UK.
- Ma, Y., & Zhu, D. Z. (2014). Improving sediment removal in standard stormwater sumps. *Water Science & Technology*, 69(10).
- Macke, E. (1982). About sedimentation at low concentrations in partly filled pipes. *Mitteilungen, Leichtweiß-Institut für Wasserbau der Technischen, Universität Braunschweig*.
- May, R. W. P. (1993) Sediment transport in pipes and sewers with deposited beds. Technical Report, Hydraulic Research Ltd., Report S No. R 320, Wallingford.
- May, R. W. P., Brown, P. M., Hare, G. R., & Jones, K. D. (1989). Self-cleansing conditions for sewers carrying sediment. Hydraulic Research Station Report SR 221.
- Mayerle, R. (1988). Sediment transport in rigid boundary channels. PhD thesis. University of Newcastle upon Tyne, England.
- Nalluri, C. and Kithsiri, M. M. A. U. (1992) Extended data on sediment transport in rigid bed rectangular channels. *J Hydraul Res* 30(6):851–856.
- Novak, P. and Nalluri, C. (1975) Sediment transport in smooth fixed bed channels. *Journal of Hydraul Division ASCE* 101(HY9):1139–1154.
- Novak, P. and Nalluri, C. (1984) Incipient motion of sediment particles over fixed beds. *Journal of Hydraulic Research* 22(3), 181 - 197.
- Ojo, S. I. A. (1980) Predictive formula for sediment discharge in a rectangular flume. Symposium on River Eng. and its Interaction with Hydrological and Hydraulic Research, IAHR, Belgrade.

- Ota, J. J., & Nalluri, C. (2003). Urban storm sewer design: Approach in consideration of sediments. *Journal of Hydraulic Engineering*, 129(4), 291-297.
- Ota, J. J., & Perrusquía, G. S. (2013). Particle velocity and sediment transport at the limit of deposition in sewers. *Water Science and Technology*, 67(5), 959-967.
- Perrusquía, G. & Nalluri, C. (1995). Modelling of bed-load transport in pipe channels. *Proc. Int. Conf. On the transport and sedimentation of solid particles*. Prague.
- Perrusquía, G. (1991). Bedload Transport in Storm Sewers. *Stream Traction in Pipe Channels*.
- Reader-Harris, M. (2015). Orifice Discharge Coefficient. In *Orifice Plates and Venturi Tubes* (pp. 127-186). Springer International Publishing.
- Rijin, L. V. (1984). Part II: Suspended load transport. *Journal of Hydraulic Engineering*, 111.
- Roesner, L. A., & Kidner, E. M. (2007). Improved protocol for classification and analysis of storm-borne solids. *Proceedings of the Water Environment Federation*, 2007(13), 5539-5566.
- Safari, M. J. S., Mohammadi, M., & Gilanizadehdizaj, G. (2013). Investigation on incipient deposition and incipient motion of sediment particles in rigid boundary channels. *Water Soil Sci Autumn*, 23(3), 13-25.
- Safari, M. J. S., Aksoy, H., & Mohammadi, M. (2015). Incipient deposition of sediment in rigid boundary open channels. *Environmental Fluid Mechanics*, 1-16.
- Sansalone, J. J., Koran, J. M., Smithson, J. A., & Buchberger, S. G. (1998). Physical characteristics of urban roadway solids transported during rain events. *Journal of Environmental Engineering*, 124(5), 427-440.
- Sartor, J. D., Boyd, G. B., & Agardy, F. J. (1974). Water pollution aspects of street surface contaminants. *Journal (Water Pollution Control Federation)*, 458-467.

- Schlutter, F., & Schaarup-Jensen, K. (1998). Sediment transport under dry weather conditions in a small sewer system. *Water Science and Technology*, 37(1), 155-162.
- Selbig, W. R., & Bannerman, R. T. (2011). Characterizing the size distribution of particles in urban stormwater by use of fixed-point sample-collection methods. Madison; U.S. Geological Survey.
- Shields, A. (1936). Application of similarity principles and turbulence research to bed-load movement. Soil Conservation Service.
- Shimatani, Y., Kanba, H., & Sakakibara, T. (1989). Proceeding of Environ. & Sani. Eng. Research, 25(0), 139-148.
- USEPA. (1986). Detention basin analysis study. Washington, D.C.
- USEPA. (1993). Natural wetlands and urban stormwater: Potential impacts and management. Washington: United States Environmental Protection Agency.
- USEPA. (1999). Sewer cleaning and inspection. EPA proceeding, 832-F-99-031.
- Vanoni, V. A. (2006). Sedimentation engineering. ASCE.
- Vaze, J., & Chiew, F. H. (2004). Study of pollutant wash off from small impervious experimental plots. *Water Resources Research*, 39(6).
- Vignoles, M., & Herremans, L. (1995). Metal pollution of sediments contained in runoff water in the Toulouse city. *Novatech* Vol. 95, No. 2, pp. 611-614.
- Wentworth, C.K. (1922) A scale of grade and class terms for clastic sediments: *Journal of Geology*, v. 30, p. 377-392.
- Wilson, M. A., Mohseni, O. M., Gulliver, J., Hozalski, R. M. & Stefan, H. G. (2009). Assessment of hydrodynamic separators for storm-water treatment. *Journal of Hydraulic Engineering* – ASCE 135 (5), 383–392.

Yalkowsky, S. H., & Bolton, S. (1990). Particle size and content uniformity. *Pharmaceutical research*, 7(9), 962-966.